FINAL TECHNICAL REPORT

for

X-RAY LASER

NRL Contract No. N00014-88-K-2029

August 1, 1988 - January 31, 1991

Principal Investigators

Norman Rostoker and Amnon Fisher

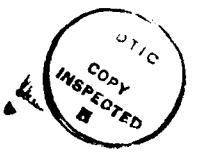

Department of Physics

University of California

Irvine, California 92717

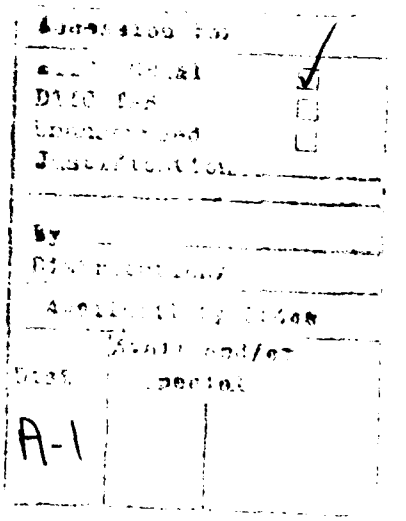

TABLE OF CONTENTS

X-RAY LASER BASED ON A Z-Θ PINCH*

F.J. Wessel, T-F Chang and N. Rostoker
University of California, Irvine, CA 92717

A. Fisher
Naval Research Laboratories, Washington, DC 20375-5000

*Supported in part by SDIO/IS and DNA.

ABSTRACT

X-Ray lasers have been developed using the Nova Laser facility to explode a thin foil. The necessary non-equilibrium condition is typically reached by rapid expansion of a small heated plasma. Plasma conditions for Ne-like or Ni-like inversion schemes are density 10^{20}-10^{21} cm^{-3} and temperature .8 - 1 keV. For H-like, He-like or Li-like schemes population inversion has been achieved by recombination and photo-resonant pumping at 10^{18} - 10^{19} cm^{-3} and .1 - .5 keV. These plasma conditions have been achieved with a Z-pinch, but so far this technique has been unsuccessful. We believe that this is because the Z-pinch always produces a non-uniform plasma. A considerable improvement should be possible with a Θ-pinch which can be produced with the same device by using an annular Z-pinch to compress a trapped axial magnetic field and a second cylindrical plasma generated on the axis.

I. INTRODUCTION :

The "neon-like" x-ray lasers require a plasma density of 10^{20} - 10^{21} electrons/cm^3 and temperature .8-1 keV. The plasma is produced in general by irradiation of a foil or fiber with a high power laser pulse followed by rapid cooling by radiation or expansion. A confining magnetic field improves the control over density.

Besides achieving the proper ionization and population inversion the plasma must be uniform enough to support laser beam propagation. The plasma created by a high power laser pulse of long wavelength (1-10μ) has satisfied these requirements. It is also possible to create a plasma by the pinch effect with the appropriate density and temperature and in a state of rapid cooling by radiation losses and/or expansion. There have been research programs during the past 10 years which attempt to produce a soft x-ray by means of a z-pinch at Physics International Co., Sandia Laboratories and Naval Research Laboratories. None of these efforts have been successful, presumably because pinch instabilities make the plasma too non-uniform for proper beam propagation.

A Θ-pinch has been suggested[1] which is inherently more stable then a Z-pinch; however the efficiency of the Θ-pinch[2] is much lower making it difficult to achieve the necessary plasma density and temperature with the available pulse power equipment. Recently the Z-Θ-pinch has been proposed[3] which appears to solve this problem. It is illustrated in Fig. 1. A slow Bz field is applied before an annular Z-pinch takes place. When the Z-pinch takes place the flux $\pi r^2 Bz$ is conserved; r is the inner radius of the annular Z-pinch. Therefore Bz increases as illustrated in Fig. 2. Measurements at UCI by Faraday[4] rotation shows that Bz reaches 1.6 M-gauss, Fig. 3, and this was with a 6 kJ capacitor bank for the driver. With a large pulse power system Bz fields as large as 40 M-gauss have been reported.[5]

1. N. Pereira, Maxwell Laboratories Memorandum, March 1983.
2. J. Katzenstein. J. Appl. Phys. 52, 676, 1981.
3. H.V. Rahman, F.J. Wessel, A. Fisher and N. Rostoker, Bull. Am. Phys. Soc. 32, 1818, 1987.
4. F.J. Wessel et al., Appl. Phys. Lett. 48, 1119, 1986.
   Rev. Sci. Inst. 57, 2247, 1986.
5. F.S. Felber et al., Phys. Fluids, 31, 2053 ,1988.

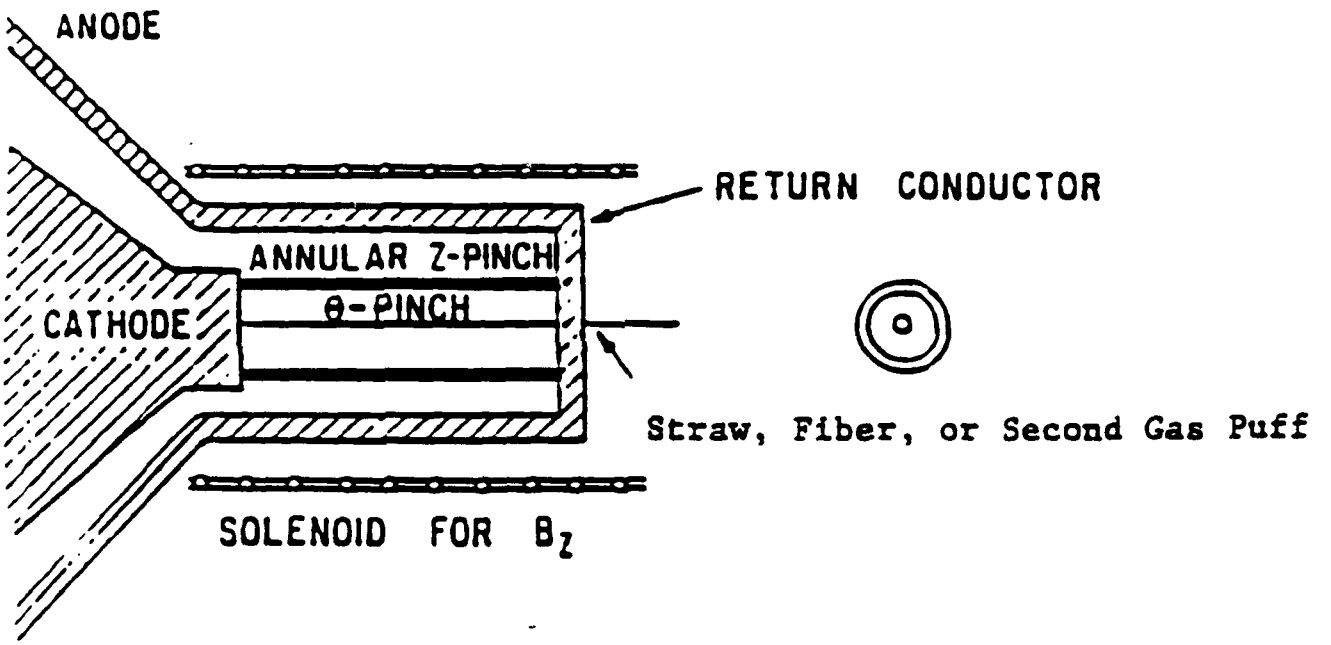

Fig. 1. Z-Θ Pinch configuration.

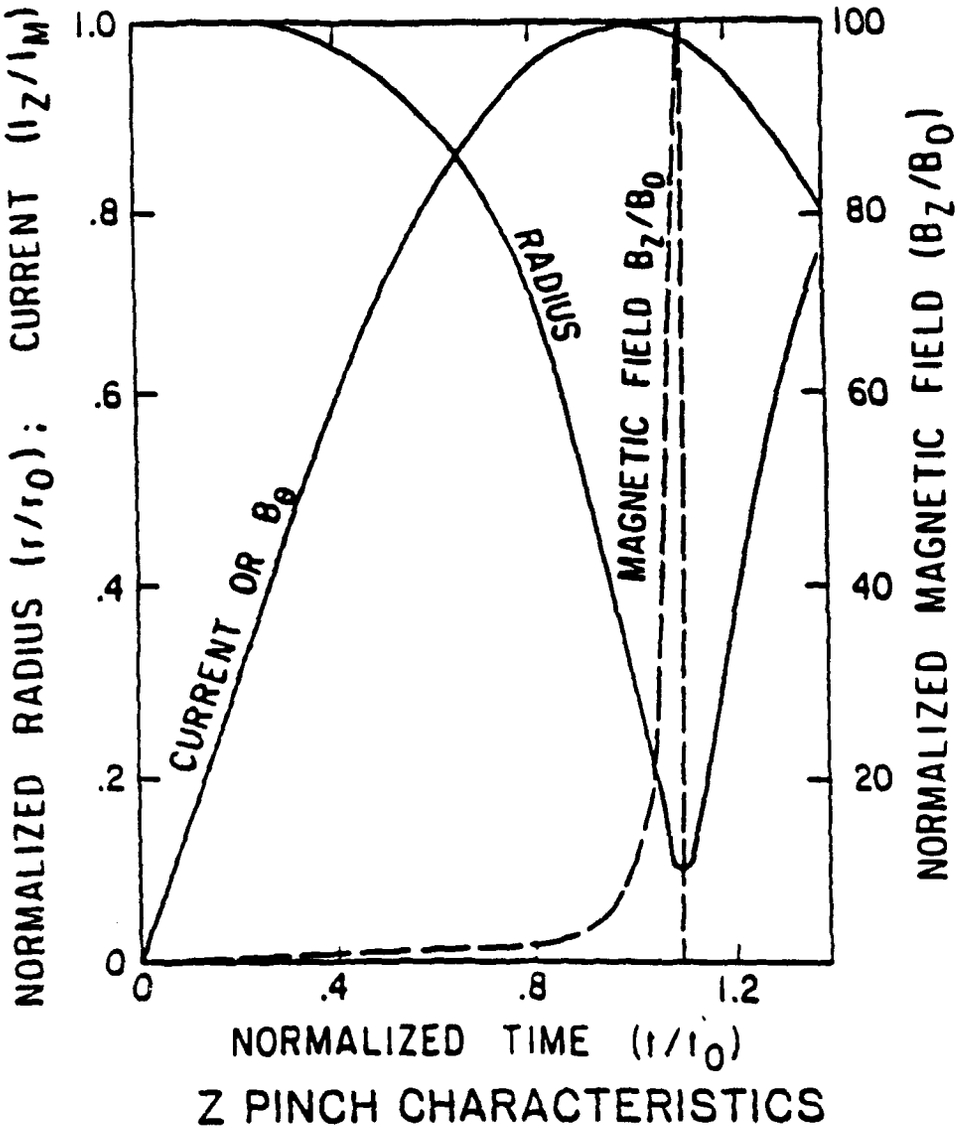
NORMALIZED RADIUS (r/r0); CURRENT (Iz/IM)
NORMALIZED MAGNETIC FIELD (Bz/B0)
NORMALIZED TIME (t/t0)
CURRENT OR Bθ
RADIUS
MAGNETIC FIELD Bz/B0
1.0
.8
.6
.4
.2
0
100
80
60
40
20
0
.4
.8
1.2
Z PINCH CHARACTERISTICS

Fig. 2.

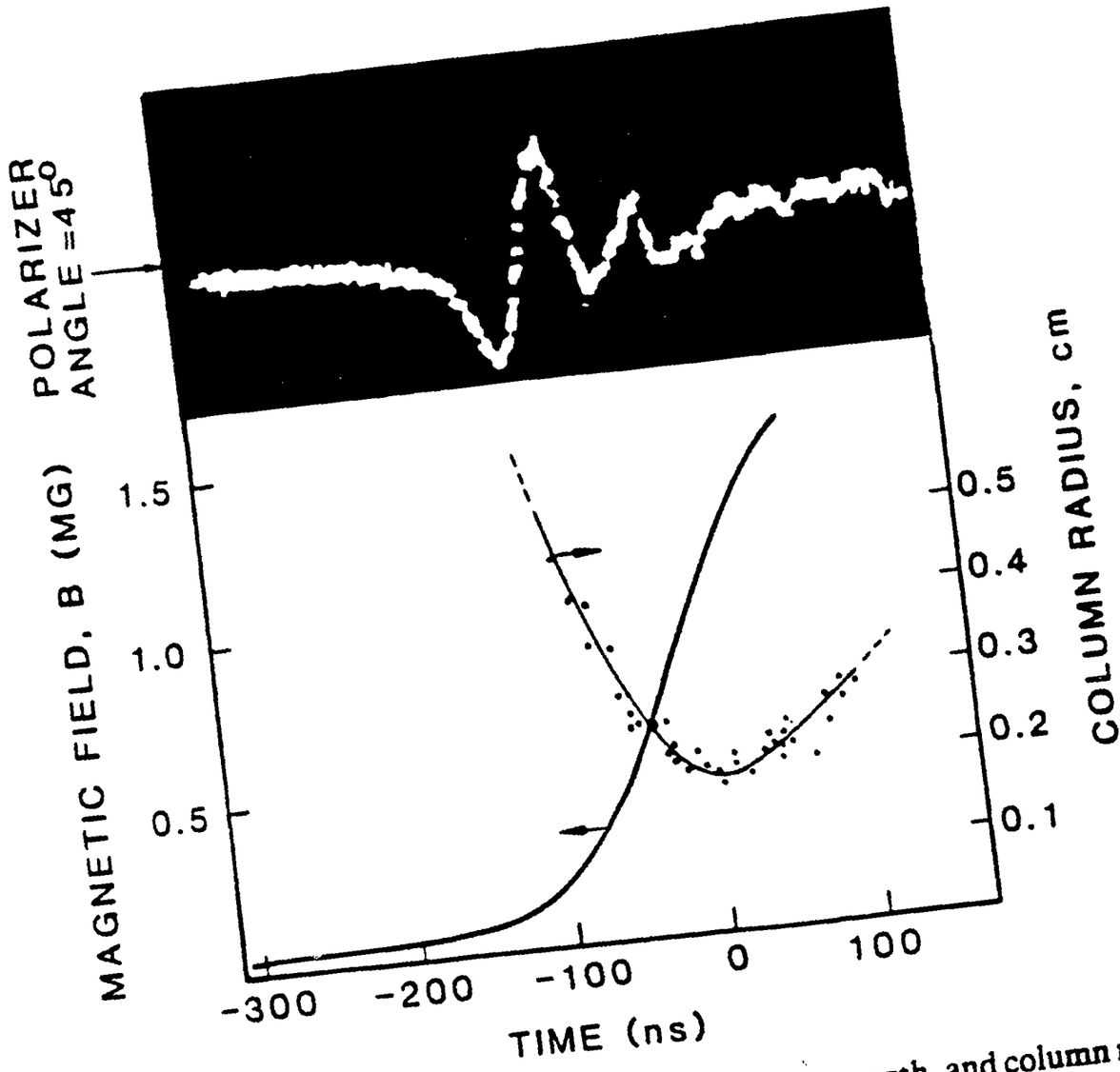

FIG. 3. Faraday rotation trace, compressed field strength, and column radius vs time. Pinch parameters: krypton, $B_0 = 9$ kG, $r_0 = 2$ cm.

II. DIAGNOSTICS:

The diagnostics include di/dt coil, soft x -ray diode, N_2 laser interferogram and laser Schlieren photography. The di/dt coil is a one turn coil cast in epoxy mounted on the vacuum chamber wall 7.5 cm from the z axis. Its signal is proportional to the time derivative of the current, di/dt. From the signal we can estimate the timing of the maximum compression.

The x-ray diode is composited by a thin filter, a mesh screen as anode, and a metal cylinder photodiode as cathode. The soft x-ray diode, with a ~2 μm mylar filter and 0.37 cm^2 Ni cathode, detects the x- ray <1keV. The hard x-ray diode, with a 13 μm saran filter and Ni cathode, detects the x-ray >1keV. The diode is placed 85 cm from the plasma axis at the end of an extended tube.

III. EXPERIMENTS :

1. PUFF WITH STRAW Z-Θ–PINCH:

The schematic diagram of the UCI puff with straw Z-Θ-pinch machine is described in the figure 4 and the straw is described in figure 5. The experiment was driven by a 30 kV, 12 μf capacitor bank. The plenum pressures used for Kr was 80 PSIG.

Fig. 6 shows the set up for Schlieren system. Schlieren photographs taken of the straw at various times during the implosion of the Z-pinch, Fig. 7, revealed the presence of a highly uniform plasma with a steep density gradient at the location of the straw. The uniformity of the Θ-pinch is observed despite any non-uniformities in the Z-pinch.

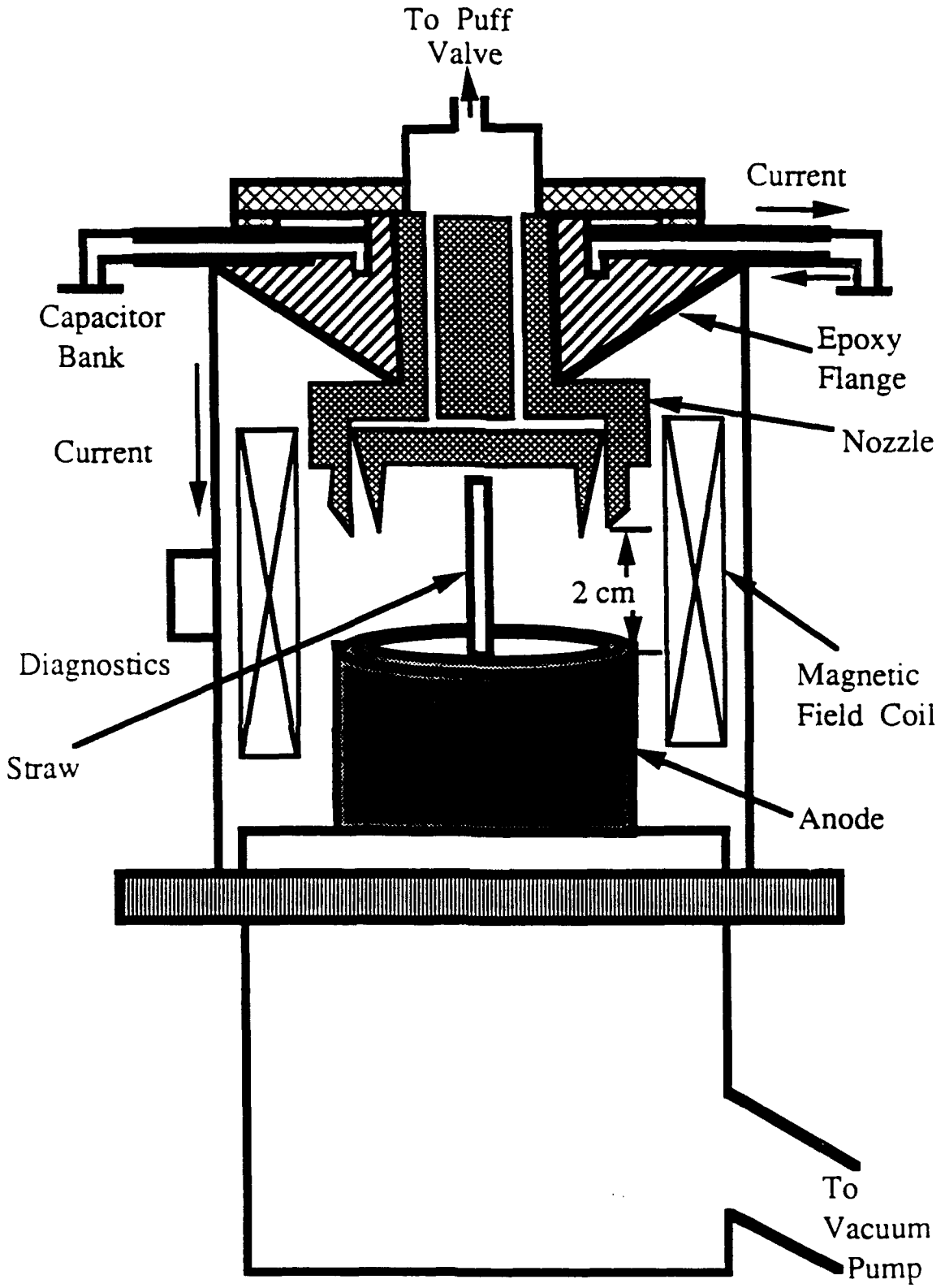

FIG. 4. Schematic Diagram of the UCI Z–Θ Pinch Machine

2μm Paralene Soda Straws coated
with NaF (0.75μm)
(Straws are provided by T. Nash at Physics International)

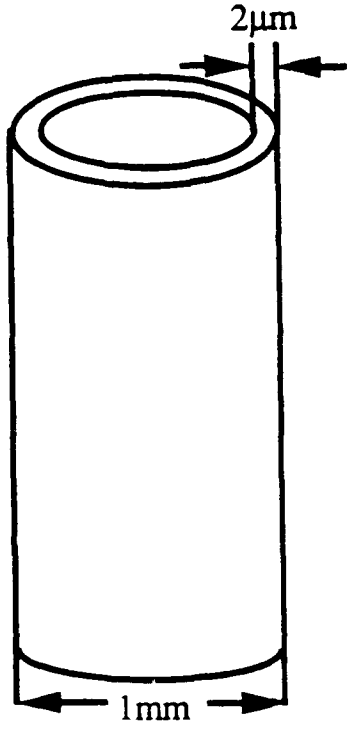

FIG. 5. Straw Description

SET UP FOR SCHIEREN SYSTEM

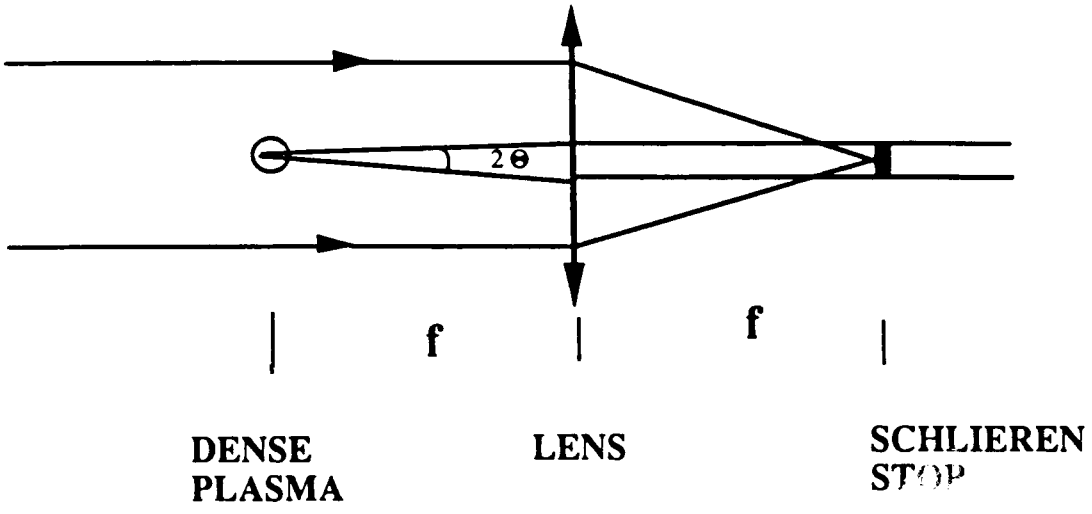

λ-337 nm

$\theta = -5.09\times10^{-23}\ \overline{\nabla n}\times\Delta l$

Stop - 1mm wide

f - 56 cm

For Visible Fringe : $\overline{\nabla n}\times\Delta l > 1.8\times10^{19}\ cm^{-3}$

Fig. 6. Set Up For Schieren System

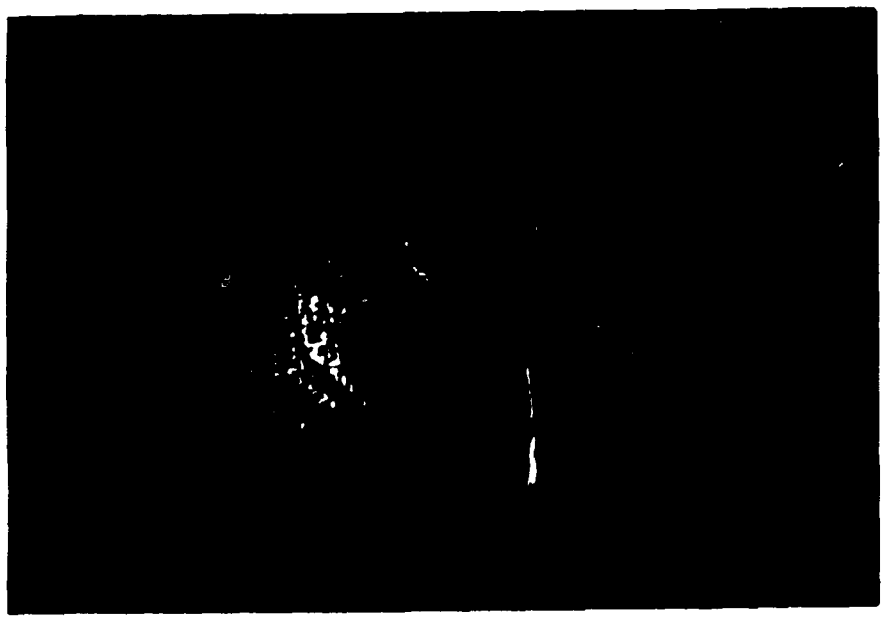

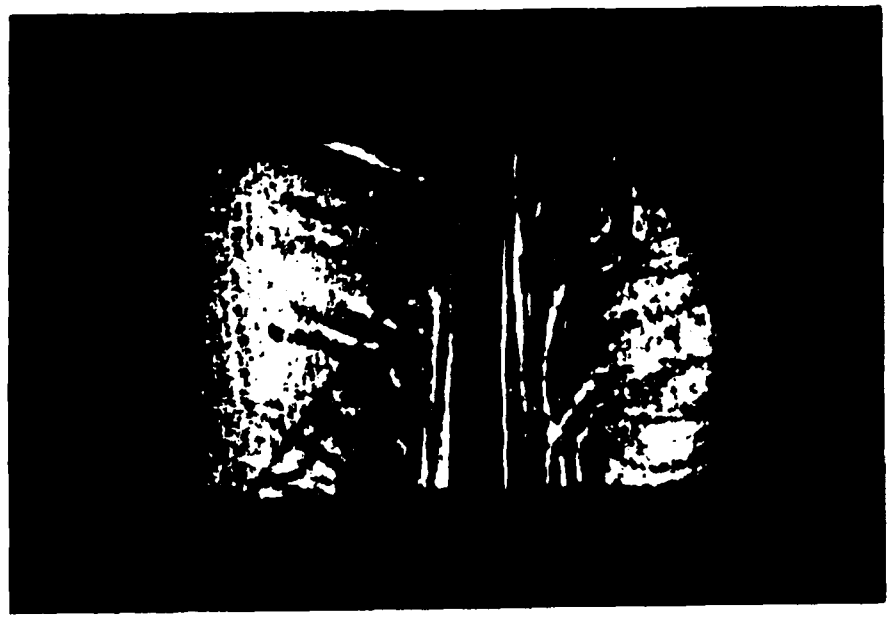

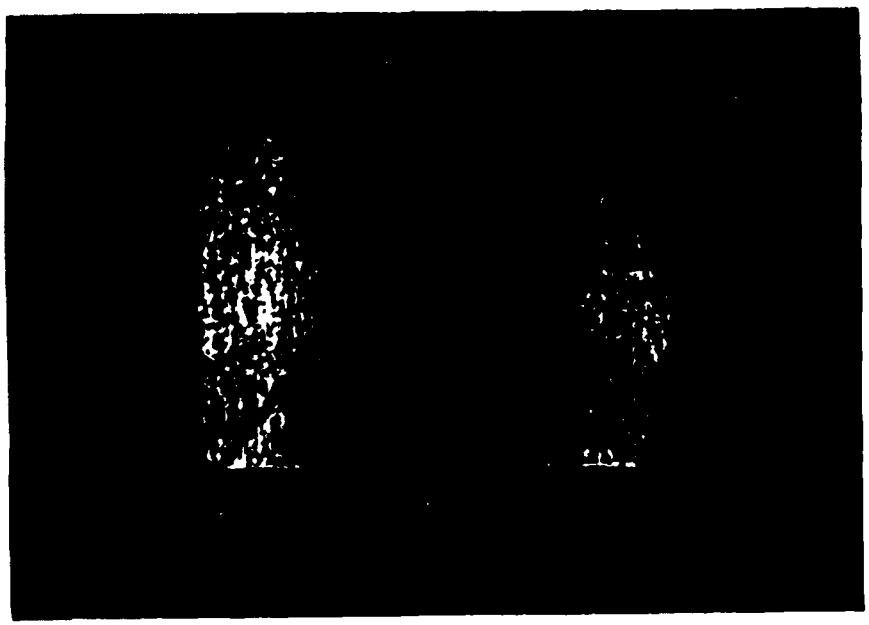

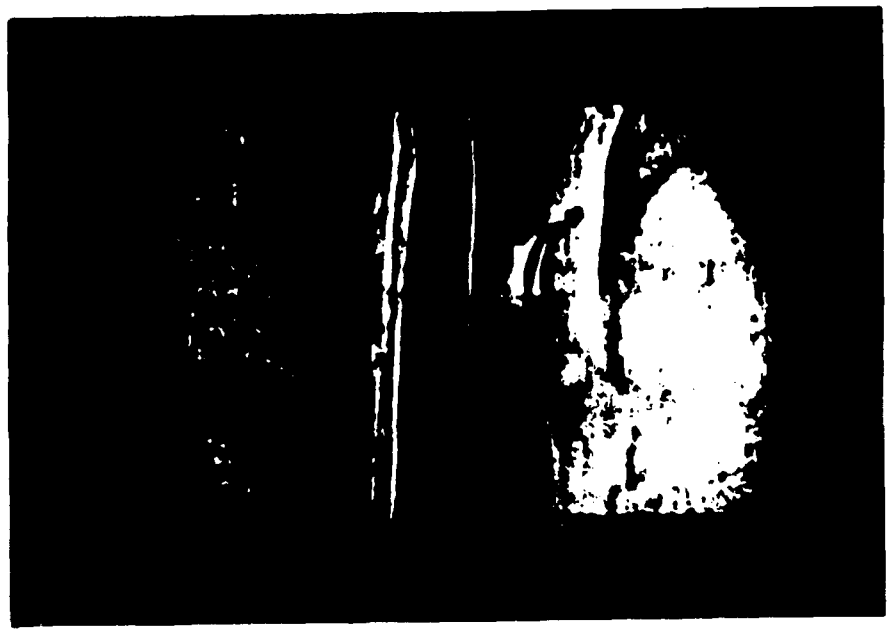

X-Ray Laser Gain from Bragg Reflection in Relativistic Electron Beam Channel Radiation Systems

M. Strauss
P. Amendt
N. Rostoker
A. Ron

Reprinted from
IEEE TRANSACTIONS ON PLASMA SCIENCE
Vol. 16, No. 5, October 1988

X-Ray Laser Gain from Bragg Reflection in Relativistic Electron Beam Channel Radiation Systems

M. STRAUSS, P. AMENDT, N. ROSTOKER, AND A. RON

Abstract—**The application of distributed feedback by Bragg reflections in electron beam channeling X-ray lasers is investigated. Expressions for low threshold gain are derived for this cavity mirror structure in single crystals and are shown to have possible application in reducing beam high-current requirements by many orders of magnitude.**

I. Introduction

RELATIVISTIC electrons propagating through axial and planar crystal channels may populate bound transverse energy eigenstates [1]–[3]. Spontaneous transitions between these states have been shown experimentally to yield narrow width, strongly forward-peaked, tunable X-ray radiation in excess of atomic bremsstrahlung radiation by an order of magnitude [4], [5]. The possibility of using the channeling mechanism as a coherent X-ray source depends on future progress in these areas: 1) achieving significant population inversion, 2) increasing the coherence length for channeling particles, and 3) creating sufficient gain from induced emission. This paper addresses the third issue, relating to the identification of an efficient mechanism for gain optimization in crystal channeling. Recent estimates suggest that even modest gains for short coherence length systems (10 μm) may require currents of the order of MA/cm^2 range for energies near 10 MeV [6]–[8]; this requirement is beyond the limit of present capabilities of high-current technology. Our aim here is to suggest a scheme to reduce the necessary currents by many orders of magnitude, thereby bringing one aspect of the channeling X-ray laser closer to experimental realization.

The concept of a distributed feedback laser in the optical range for atomic emitters has been proposed by Kogelnik and Shank [9] and was later extended to the X-ray range [10], [11]. The feedback mechanism is supplied by multiple Bragg reflections from periodic perturbations of the crystalline refractive index. Some advantages to using distributed feedback (DFB) include the intrinsic compactness and high degree of spectral selectivity available without the need for cavity mirrors [9]–[11]. Our purpose here is to apply DFB techniques for significantly reducing the spatial gain requirements in projected coherent X-ray channeling experiments.

The use of DFB X-ray lasers in channeled relativistic beam systems differs in two respects from atomic DFB lasers. First, the radiation in the forward direction emitted by the relativistic beam is Doppler up-shifted to the X-ray range, while the backward reflected radiation is Doppler down-shifted relative to the beam. Thus, amplification occurs only in the beam direction, leaving an asymmetric X-ray intensity distribution. This feature represents the main differences between our channeling DFB analysis and the atomic coupled wave theory of DFB lasers [9]. Secondly, the channeling DFB has a significant advantage in radiation tunability. By adjusting the electron beam energy, the Doppler up-shifted radiation can be tuned with high precision (≤ 1 percent) onto a line in the DFB mode spectrum near the Bragg reflection frequency.

II. Analysis of DFB X-Ray Laser

As illustrated in Fig. 1, we begin by characterizing the set of channeling transverse eigenstates as a two-level system with states $|1\rangle$ and $|2\rangle$, where W and $\hbar\omega_n = \epsilon_2 - \epsilon_1$ are the population and energy differences, respectively. The directions of beam channeling and Bragg reflections are taken in the z direction, as illustrated in Fig. 2. The electric E and polarization P fields are taken in the transverse x direction and are defined in terms of forward and backward traveling waves:

$$E(z, t) = \epsilon_+(z, t)\, e^{-i\omega(t - z/c)} + \epsilon_-(z, t)\, e^{-i\omega(t + z/c)} + \text{c. c.}$$

$$P(z, t) = p_+(z, t)\, e^{-i\omega(t - z/c)} + p_-(z, t)\, e^{-i\omega(t + z/c)} + \text{c. c.}$$

where ω is the electromagnetic wave frequency, c is the speed of light, $\epsilon_\pm$ and $p_\pm$ are slowly varying complex amplitudes, and transverse field effects are not considered. The behavior of $p_\pm$ is readily determined from a density

Manuscript received January 25, 1988, revised April 27, 1988.

M. Strauss was with the Department of Physics, University of California, Irvine. He is now with the Department of Physics, Nuclear Research Center-Negev, P.O. Box 9001, Beer-Sheva, Israel.

P. Amendt was with the Department of Physics, University of California, Irvine. He is now with SISSA, Strada Costiera 11, Trieste, Italy.

N. Rostoker is with the Department of Physics, University of California, Irvine, CA 92717.

A. Ron was with the Department of Physics, University of California, Irvine. He is now with the Department of Physics, Technion, Haifa, Israel.

IEEE Log Number 8823059

0093-3813/88/1000-0548$01.00 © 1988 IEEE

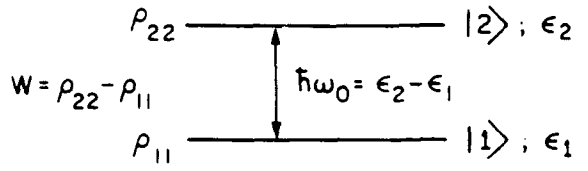

Fig. 1. Two-level model.

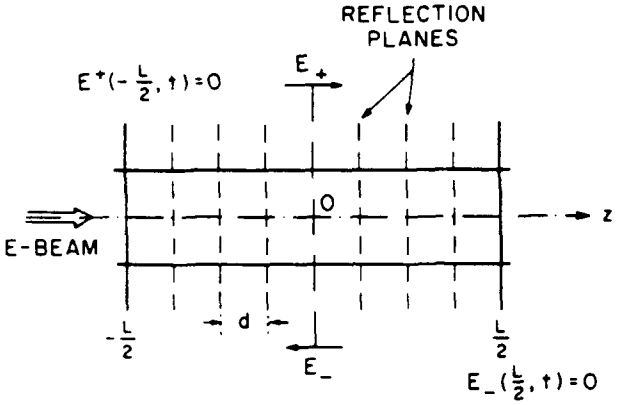

Fig. 2. Channel radiation and Bragg reflection ($E(z, t) = E_+(z, t) + E_-(z, t)$).

matrix approach and obeys the Bloch equation [7], [12]:

$$\frac{\partial}{\partial t} p_\pm + v \frac{\partial}{\partial z} p_\pm = i\Delta_\pm p_\pm - i(1 \mp v/c) d^2 n_b W \epsilon_\pm / \hbar - \Gamma p_\pm \tag{1}$$

where v is the channeling electron speed in the z direction, d is the electric dipole moment $e\langle 1| \times |2\rangle$, n_b is the beam number density, $\hbar$ is Planck's constant, Γ is a phenomenological damping constant related to the channeling coherence length v/Γ, $\Delta_\pm = \omega(1 \mp v/c) - \omega_o$ is a detuning frequency, and the factor v/c represents a magnetic dipole interaction correction [7]. We note that $\Delta_\pm = 0$ defines the channeling resonance condition, giving a Doppler up-shifted frequency $\omega = \omega_o/(1 - v/c) \simeq 2\gamma^2\omega_o$ in the forward direction (Δ_+) and a reduced frequency $\omega = \omega_o/(1 + v/c) \simeq \omega_o/2$ in the backward direction (Δ_-). Typically, $\hbar\omega_o$ is a few electron volts in the laboratory frame so that for the relativistic factor γ on the order of 20, $\hbar\omega$ is on the order of several keV. In this range of energies, ω may be chosen to closely match the first-order Bragg frequency $\omega_B \equiv \pi c/a$, where a is the periodic reflection plane spacing. Consequently, the channeling electron energy may be tuned to satisfy the Bragg reflection condition and induce distributed feedback in the channeling crystal.

Equation (1) must be supplemented by Maxwell's wave equation for the electric field:

$$\frac{\partial^2}{\partial z^2} \underline{E} - \frac{1}{c^2} \frac{\partial^2}{\partial t^2} \underline{E} = \frac{4\pi}{c^2} \frac{\partial}{\partial t} \left(\frac{\partial}{\partial t} \underline{P} + c\nabla \times \underline{M} + \underline{J} \right) \tag{2}$$

where the polarization $\underline{P}$ and magnetization $\underline{M} = \underline{P} \times \underline{v}/c$ are due to the beam electrons [7]. In (2) $\underline{J}$ is the crystal-induced current of the bound electrons. We approximate $\underline{J} = n_e e \underline{v}_e$ and $\partial/\partial t\, \underline{J} = e^2 n_e \underline{E}/m_e$, where the spatial modulation of the atomic electron density $n_e(z) = n_o \cos(2\omega_B z/c)$ provides coupling between the forward and backward propagating waves [9], [10]. In the slowly varying envelope approximation (2) can be written as

$$\frac{1}{c}\frac{\partial}{\partial t}\epsilon_\pm \pm \frac{\partial}{\partial z}\epsilon_\pm = \frac{2\pi i}{c\omega}\left[\omega^2(1 \mp v/c)p_\pm - \frac{n_o e^2}{2m}\epsilon_\mp e^{\pm 2i(\omega_B - \omega)z/c}\right]. \tag{3}$$

Decoupling of (1), (3) can be accomplished as follows. In the limit of small coherence lengths v/Γ, i.e., $\Gamma \gg v((\partial/\partial z(p_\pm))/p_\pm, ((\partial/\partial t)p_\pm)/p_\pm$ and (1) simplifies: $p_\pm = id n_b W(d\epsilon_\pm/\hbar)(1 \mp v/c)/(i\Delta_\pm - \Gamma)$. Near resonance, i.e., $\omega \sim 2\gamma^2\omega_o$ and $\Delta_+/\Gamma \ll 1$, giving

$$p_+ = -id^2 n_b W \epsilon_+ (1 - v/c)\hbar\Gamma. \tag{4}$$

In this limit $\Delta_- \sim \omega$, $\Delta_- \gg \Gamma$ and in the case of low gain p_- can be ignored in (3). We now define the scalar gain $g = 2\pi\omega d_1^2 n_b W/\hbar c\Gamma$, where $d_1 = d(1 - v/c)$ and n_b is the beam density. Substituting (4) in (3) and redefining $\epsilon_\pm$ as $\epsilon_\pm \exp(\pm iz(\omega_B - \omega)/c)$, we obtain

$$\pm\frac{\partial}{\partial z}\epsilon_\pm + \frac{1}{c}\frac{\partial}{\partial t}\epsilon_\pm + i\delta\epsilon_\pm + i\kappa\epsilon_\mp = g_\pm e_\pm \tag{5}$$

where $g_+ = g$, $g_- = 0$, $\kappa = \pi n_o e^2/cm_e\omega$ and $\delta = (\omega_B - \omega)/c$.

We now find steady-state solutions appropriate for the system at threshold [9]. Using (5),

$$\frac{d}{dz}\epsilon_+ - (g_+ - i\delta)\epsilon_- + i\kappa\epsilon_- = 0 \tag{6}$$

$$-\frac{d}{dz}\epsilon_- - (g_- - i\delta)\epsilon_- + i\kappa\epsilon_+ = 0 \tag{7}$$

where g is identified as a threshold gain. To include radiation losses in (6) and (7), $g_\pm \to g_\pm - g_{los}$, where g_{los} is the radiation loss factor, and for simplicity is ignored in the equations below. Notice that (6) and (7) differ from the corresponding equations in [9] due to the fact that beam electrons produce gain only in the forward direction. The anisotropy ($g_+ \neq g_-$) forces p_- to be negligibly small.

The coupled wave equations ((6), (7)) describe the spatial variation of transmitted and reflected wave amplitudes in a beam channeling DFB medium. For a slab of length L centered at $z = 0$, the accompanying boundary conditions read $\epsilon_+(-L/2) = \epsilon_-(L/2) = 0$ and no external radiation sources are assumed. The corresponding eigenvalue solutions to (6) and (7) are found directly:

$$\epsilon_+(z) = e^{gz/2}\sinh[\lambda(z + L/2)]$$
$$\epsilon_-(z) = \pm e^{gz/2}\sinh[\lambda(z - L/2)] \tag{8}$$

where $\lambda = [(g/2 - i\delta)^2 + \kappa^2]^{1/2}$ and the dispersion relation is

$$\left(\lambda - \frac{g}{2} + i\delta\right) + \left(\lambda + \frac{g}{2} - i\delta\right) e^{-2\lambda L} = 0. \quad (9)$$

The allowed resonance frequencies δ and threshold values g can be obtained from (9). A formal solution of (9) is

$$\lambda = \pm i\kappa \sinh(\lambda L) \quad (10)$$

$$\frac{g}{2} - i\delta = \mp i\kappa \cosh(\lambda L). \quad (11)$$

Equation (10) determines λ for given κ and L. Substitution of λ into (11) and equating real and imaginary parts yields the allowed δ and g.

Equations (10) and (11) are transcendental equations requiring numerical solutions in general [9]. Approximate formulas can be obtained in the limit of strong reflections: $(\kappa L)^2 >> (gL)^2 + 1$ and $\lambda L << 1$. Upon expanding (10) in this limit and using the expression for λ, we find, for the first resonance,

$$\delta \simeq \kappa \quad (12)$$

and the threshold gain condition g_t is

$$g_t \simeq 6/\kappa^2 L^3. \quad (13)$$

Typically, $\kappa \sim \pi n_o e^2/m_e c\omega_B$ is on the order of 5×10^3 cm^{-1} in a number of crystalline samples used in channeling studies, e.g., silicon and diamond, where n_o is approximately the crystal-bound electron density. For $L \sim 0.1$ cm, then $g_t = 2 \times 10^{-4}$ cm^{-1} and low threshold values can be obtained in beam channeled DFB techniques. For the case where the gain g is larger than the threshold gain g_t, the radiation fields $\epsilon_\pm$ increase with time as exp $[(g - g_t)ct/2]$ in the linear range. Thus an amplification factor $(g - g_t)ct/2 \sim 1$ is obtained for a beam pulse duration of 50 ns in $L = 0.1$ cm for $g \sim 10^{-3}$ cm^{-1}. This result should be compared to the gain $gL \sim 1$ obtained in a one passage amplification (with no reflections), wherefore $L = 0.1$ cm, $g \sim 10$ cm^{-1}. The DFB mechanism in beam channeling has a possible application of reducing current density requirements by many orders of magnitude.

In the present treatment we have neglected radiation losses (g_{los}). It is possible in making use of Borman anomalous transmission [13]-[16] that X-ray losses can be negligibly small. In an actual experiment, the requirement of the Bragg condition would generate standing waves with nodes on the atomic sites so that the condition for the Borman effect would be fulfilled. Threshold conditions of the combined effects of the DFB mechanism and the Borman effect require further study.

III. Discussion

In order to produce radiation with $\hbar\omega \sim$ a few keV, the electron beam energy should be at least 10 MeV. Observable gain requires a current density of about 10^6 A/cm^2 without DFB, and about 10^2 A/cm^2 with DFB. In addition, the transverse beam energy (beam thermal energy prior to acceleration to 10 MeV) should be less than approximately 10 eV. The only current accelerator that meets these requirements is the Advanced Test Accelerator at the Lawrence Livermore National Laboratory, which produces a high-quality beam of current density greater than 10^3 A/cm^2 at an energy of up to 50 MeV with a pulse length of 50 ns. The modified betatron being developed at the University of California at Irvine has attained [17] 10^3 A/cm^2 at 10 MeV. However, the beam quality has not yet been evaluated. Experimental realization of an X-ray laser based on DFB and channel radiation thus appears to be feasible in terms of existing and emerging accelerator technology.

One of the concerns for such an X-ray laser is survival of the crystal. We consider heating for a beam of energy 10 MeV, 200 A/cm^2, and a 50 ns pulse. The temperature change is $\Delta T = n_b c \Delta t \Delta\epsilon_L/\rho c_v$, where $\rho = 2.5$ gm/cm^3 (density), $c_v = 0.12$ cal/gm° κ (specific heat), $n_b = 4 \times 10^{10}$/cm^3 (beam density $n_b = J/ec$ where $J = 200$ A/cm^2 is current density), $\Delta t = 50$ ns (beam pulse length), and $\Delta\epsilon_L = 0.3$ MeV/cm (electron energy loss). We have used data for carbon as an example. The result is $\Delta T = 3$ K. This is an upper bound because a channeling electron will couple less with an almost perfect crystal than is typical in a stopping power/energy loss experiment. In addition, the crystal can be cooled. Heating is a problem for constant current accelerators that are usually employed for channel radiation measurements, but is evidently not a problem for a 50 ns beam pulse.

The coherence length is v/Γ and is typically 10-100 μm in experiments on spontaneous channel radiation [1]. After this distance an electron leaves the channel and no longer contributes to the radiation. It may be possible to increase this length by cooling the crystal. This would make the experimental realization of gain much easier and increase the efficiency. From channeling radiation experiments in silicon and diamond, the photon production is 10^{-3} photons/electron-cm in a 10 percent bandwidth in an angle of a few millirad. This means approximately 10^{-5} photons/electron or an energy efficiency of about 10^{-8}. For currents of 0.1 mA, beam radius of 0.5 cm, and a 20 μm thick crystal, 10^{10} photons/s were produced. If we assume a current of 200 A, about 2×10^{16} photons/s would be produced, or 10^9 photons from a 50 ns pulse. Measurements to evaluate the DFB X-ray laser are thus feasible whether or not the coherence length can be increased.

Acknowledgment

The authors acknowledge the usefulness of their discussions with Prof. A. Fisher.

References

[1] J. U. Andersen, E. Bonderup, and R. H. Pantell, *Ann. Rev. Nucl. Part. Sci.*, vol. 33, p. 453, 1983.
[2] V. V. Beloshitsky and F. F. Komarov, *Phys. Repts.*, vol. 93, p. 117, 1982.

[3] G. Kunzki and J. K. McIver, *Phys. Rev. B*, vol. 32, p. 4358, 1985.
[4] R. K. Klein *et al.*, *Phys. Rev. B*, vol. 31, p. 68, 1985.
[5] B. L. Berman *et al.*, *Nucl. Instrum. Methods B*, vol. 10/11, p. 611, 1985.
[6] V. V. Beloshitsky and M. A. Kumakhov, *Phys. Lett.*, vol. 69a, p. 247, 1978.
[7] G. Kunzki, M. Strauss, J. Oreg, and N. Rostoker, *Phys. Rev. A*, vol. 35, p. 3424, 1987.
[8] Y. H. Ohtsuki, *Nucl. Instrum. Methods B*, vol. 2, p. 80, 1984.
[9] H. Kogelnik and C. V. Shank, *Appl. Phys. Lett.*, vol. 18, p. 152, 1971; *J. Appl. Phys.*, vol. 43, p. 2327, 1972.
[10] A. Yariv, *Appl. Phys. Lett.*, vol. 25, p. 105, 1974.
[11] R. A. Fisher, *Appl. Phys. Lett.*, vol. 24, p. 598, 1974.
[12] M. Strauss, P. Amendt, H. U. Rahman, and N. Rostoker, *Phys. Rev. Lett.*, vol. 55, p. 406, 1985.
[13] B. W. Batterman, *Rev. Mod. Phys.*, vol. 36, p. 681, 1964.
[14] B. Borie, *Acta Crystallogr.*, vol. 21, p. 470, 1966.
[15] E. J. Saccocio and A. Zajac, *Phys. Rev.*, vol. 139, p. 225, 1965.
[16] J. P. Hannon and G. T. Trammell, *Opt. Com.*, vol. 15, p. 330, 1975.
[17] B. Mandelbaum, H. Ishizuka, A. Fisher, and N. Rostoker, presented at the *6th Int. Conf. on High Power Particle Beams, BEAMS '86*, Kobe, Japan; to be published in *Phys. Fluids*.
[18] R. H. Pantell *et al.*, *IEEE Trans. Nucl. Sci.*, vol. NS-30, p. 3150, 1983; R. K. Klein *et al.*, *Phys. Rev. B*, vol. 28, p. 3718, 1983.

X-ray laser gain from Bragg reflection coupling in channeled relativistic beam systems

M. Strauss
Physics Department, Nuclear Research Center-Negev, P. O. Box 9001, Beer-Sheva, Israel

P. Amendt[a)] and N. Rostoker
Physics Department, University of California, Irvine, California 92717

A. Ron
Physics Department, Technion, Haifa, Israel

(Received 5 October 1987; accepted for publication 4 January 1988)

The application of distributed feedback by Bragg reflections in electron beam channeling x-ray lasers is investigated. Expressions for low threshold gain are derived for this cavity mirror structure in single crystals and are shown to have possible application in reducing beam high current requirements by many orders of magnitude.

Relativistic electrons propagating through axial and planar crystal channels may populate bound transverse energy eigenstates.[1-3] Spontaneous transitions between these states have been shown experimentally to yield narrow width, strongly forward-peaked, tunable x-ray radiation in excess of atomic bremsstrahlung radiation by an order of magnitude.[4,5] The possibility of using the channeling mechanism as a coherent x-ray source depends on future progress in three areas: (1) achieving significant population inversion, (2) increasing the coherence length for channeling particles, and (3) creating sufficient gain from induced emission. This letter addresses the third issue relating to the identification of an efficient mechanism for gain optimization in crystal channeling. Recent estimates suggest that even modest gains for short coherence length systems (10μ) may require currents of the order of MA/cm^2 range for energies near 10 MeV[6-8]; this requirement is in the limit of present capabilities of high current technology. Our aim here is to suggest a scheme to reduce the necessary currents by many orders of magnitude, thereby bringing one aspect of the channeling x-ray laser closer to experimental reach.

The concept of a distributed feedback laser in the optical range for atomic emitters has been proposed by Kogelnik and Sank[9] (KS) and was extended later on to the x-ray range.[10,11] The feedback mechanism is supplied by multiple Bragg reflections from periodic perturbations of the crystalline refractive index. Some advantages in using distributed feedback (DFB) include the intrinsic compactness and high degree of spectral selectivity available without the need for cavity mirrors.[9-11] Our purpose here is to apply DFB techniques to significantly reduce the spatial gain requirements in projected coherent x-ray channeling experiments.

The use of DFB x-ray lasers in channeled relativistic beam systems differs in two respects from atomic DFB lasers. First, the radiation in the forward direction emitted by the relativistic beam is Doppler up-shifted to the x-ray range, while the backward reflected radiation is Doppler down-shifted relative to the beam. Thus, amplification occurs only in the beam direction, leaving an asymmetric x-ray intensity distribution. This feature represents the main difference between our channeling DFB analysis and the atomic coupled wave theory of DFB lasers by SK.[9] Second, the channeling DFB has a significant advantage in radiation tunability. By adjusting the electron beam energy, the Doppler up-shifted radiation can be tuned with high precision ($\lesssim 1\%$) onto a line in the DFB mode spectrum near the Bragg reflection frequency.

We begin by characterizing the set of channeling transverse eigenstates as a two-level system with states $|1\rangle$ and $|2\rangle$, W and $\hbar\omega_0 = \epsilon_2 - \epsilon_1$ are the population and energy differences, respectively. The directions of beam channeling and Bragg reflections are taken in the z direction. The electric E and polarization P fields are taken in the transverse x direction and are defined in terms of forward and backward traveling waves:

$$E(z,t) = \epsilon_+(z,t)e^{-i\omega(t-z/c)} + \epsilon_-(z,t)e^{-i\omega(t+z/c)} + \text{c.c.},$$

$$P(z,t) = p_+(z,t)e^{-i\omega(t-z/c)} + p_-(z,t)e^{-i\omega(t+z/c)} + \text{c.c.},$$

where ω is the electromagnetic wave frequency, c is the speed of light, $\epsilon_\pm$ and $p_\pm$ are slowly varying complex amplitudes, and transverse field effects are not considered. The behavior of $p_\pm$ is readily determined from a density matrix approach and obeys the Bloch equation[7,12]:

$$\frac{\partial}{\partial t}p_\pm + v\frac{\partial}{\partial z}p_\pm = i\Delta_\pm p_\pm - i(1\mp v/c)d^2 n_b W\epsilon_\pm/\hbar - \Gamma p_\pm, \quad (1)$$

where v is the channeling electron speed in the z direction, d is the electric dipole moment $e\langle 1|x|2\rangle$, n_b is the beam number density, $\hbar$ is Planck's constant, Γ is a phenomenological damping constant related to the channeling coherence length v/Γ, $\Delta_\pm = \omega(1\mp v/c) - \omega_0$ is a detuning frequency, and the factor v/c represents a magnetic dipole interaction correction.[7] We note that $\Delta_\pm = 0$ defines the channeling resonance condition, giving a Doppler up-shifted frequency $\omega = \omega_0/(1-v/c) \simeq 2\gamma^2\omega_0$ in the forward direction (Δ_+) and a reduced frequency $\omega = \omega_0/(1+v/c) \simeq \omega_0/2$ in the backward direction (Δ_-). Typically $\hbar\omega_0$ is a few electron volts in the laboratory frame so that for the relativistic factor γ on the order of 20, $\hbar\omega$ is on the order of several keV. In this range of energies, ω may be chosen to closely match the first order Bragg frequency $\omega_B \equiv \pi c/a$,

[a)] Present address: Sissa, Strada Costiera 11, Trieste, Italy

 0003-6951/88/110866-03$01.00

where a is the periodic reflection plane spacing. Consequently, the channeling electron energy may be tuned to satisfy the Bragg reflection condition and induce distributed feedback in the channeling crystal.

Equation (1) must be supplemented by Maxwell's wave equation for the electric field:

$$\frac{\partial^2}{\partial z^2}\mathbf{E}-\frac{1}{c^2}\frac{\partial^2}{\partial t^2}\mathbf{E}=\frac{4\pi}{c^2}\frac{\partial}{\partial t}\left(\frac{\partial}{\partial t}\mathbf{P}+c\nabla\times\mathbf{M}+\mathbf{J}\right), \quad (2)$$

where the polarization $\mathbf{P}$ and magnetization $\mathbf{M}=\mathbf{P}\times\mathbf{v}/c$ are due to the beam electrons.[7] In Eq. (2) $\mathbf{J}$ is the crystal-induced current of the bound electrons. We approximate $\mathbf{J}=n_e e\mathbf{v}_e$ and $(\partial/\partial t)\mathbf{J}=e^2 n_e\mathbf{E}/m_e$, where the spatially modulated atomic electron density $n_e(z)=n_0\cos(2\omega_B z/c)$ with n_0 on the order of the crystal bound electron density provides coupling between the forward and backward propagating waves.[9,10] In the slowly varying envelope approximation Eq. (2) can be written as

$$\frac{1}{c}\frac{\partial}{\partial t}\epsilon_\pm \pm\frac{\partial}{\partial z}\epsilon_\pm = \frac{2\pi i}{c\omega}\left[\omega^2\left(1\mp\frac{v}{c}\right)p_\pm-\frac{n_0 e^2}{2m}\epsilon_\mp e^{\pm 2i(\omega_B-\omega)z/c}\right]. \quad (3)$$

Decoupling of Eqs. (1) and (3) can be accomplished as follows. In the limit of small coherence lengths v/Γ, i.e., $\Gamma\gg v[(\partial/\partial z)p_\pm]/p_\pm$, $[(\partial/\partial t)p_\pm]/p_\pm$ and Eq. (1) simplifies: $p_\pm\simeq id n_b W(d\epsilon_\pm/\hbar)(1\mp v/c)/(i\Delta_\pm-\Gamma)$. Near resonance, i.e., $\omega\sim 2\gamma^2\omega_0$ and $\Delta_\pm/\Gamma\ll 1$, giving

$$p_+=-id^2 n_b W\epsilon_+(1-v/c)\hbar\Gamma. \quad (4)$$

In this limit $\Delta_-\sim\omega$, $\Delta_-\gg\Gamma$ and in the case of low gain p_- can be ignored in Eq. (3). We now define the scalar gain $g=2\pi\omega d_1^2 n_b W/\hbar c\Gamma$, where $d_1=d(1-v/c)$. Substituting Eq. (4) in Eq. (3) and redefining $\epsilon_\pm$ as $\epsilon_\pm\times\exp[\pm iz(\omega_B-\omega)/c]$ we obtain

$$\pm\frac{\partial}{\partial z}\epsilon_\pm+\frac{1}{c}\frac{\partial}{\partial t}\epsilon_\pm+i\delta\epsilon_\pm+i\kappa\epsilon_\mp=g_+\epsilon_\pm, \quad (5)$$

where $g_+=g$, $g_-=0$, $\kappa=\pi n_0 e^2/cm_e\omega$, and $\delta=(\omega_B-\omega)/c$.

We now find steady-state solutions appropriate for the system at threshold.[9] Using Eq. (5),

$$\frac{d}{dz}\epsilon_+-(g_+-i\delta)\epsilon_++i\kappa\epsilon_-=0, \quad (6)$$

$$-\frac{d}{dz}\epsilon_--(g_--i\delta)\epsilon_-+i\kappa\epsilon_+=0, \quad (7)$$

where g is identified as a threshold gain. To include radiation losses in Eqs. (6) and (7) $g_\pm\to g_\pm-g_{\rm loss}$, where $g_{\rm loss}$ is the radiation loss factor, and for simplicity is ignored in the following. Notice that Eqs. (6) and (7) differ from the corresponding equations of KS due to the fact that beam electrons produce gain only in the forward direction. The anisotropy $(g_+\neq g_-)$ forces p_- to be negligibly small.

The coupled wave Eqs. (6) and (7) describe the spatial variation of transmitted and reflected wave amplitudes in a beam channeling DFB medium. For a slab of length L centered at $z=0$, the accompanying boundary conditions read: $\epsilon_+(-L/2)=\epsilon_-(L/2)=0$ and no external radiation sources are assumed. The corresponding eigenvalue solutions to Eqs. (6) and (7) are found directly:

$$\epsilon_+(z)=e^{gz/2}\sinh[\lambda(z+L/2)],$$
$$\epsilon_-(z)=\pm e^{gz/2}\sinh[\lambda(z-L/2)], \quad (8)$$

where $\lambda=[(g/2-i\delta)^2+\kappa^2]^{1/2}$ and the dispersion relation is

$$(\lambda-g/2+i\delta)+(\lambda+g/2-i\delta)e^{-2\lambda L}=0. \quad (9)$$

The allowed resonance frequencies δ and threshold values g can be obtained from Eq. (9). A formal solution of Eq. (9) is

$$\lambda=\pm i\kappa\sinh(\lambda L), \quad (10)$$

$$g/2-i\delta=\mp i\kappa\cosh(\lambda L). \quad (11)$$

Equation (10) determines λ for given κ and L. Substitution of λ into Eq. (11) and equating real and imaginary parts yields the allowed δ and g.

Equations (10) and (11) are transcendental equations requiring numerical solution in general.[9] Approximate formulas can be obtained in the limit of strong reflections: $(\kappa L)^2\gg(gL)^2+1$ and $\lambda L\ll 1$. Upon expanding Eq. (10) in this limit and using the expression for λ we find for the first resonance:

$$\delta\simeq\kappa, \quad (12)$$

and the threshold gain condition g_t is

$$g_t\simeq 6/\kappa^2 L^3. \quad (13)$$

Typically $\kappa\sim\pi n_0 e^2/m_e c\omega_B$ is on the order of 5×10^3 cm^{-1} in a number of crystalline samples used in channeling studies, e.g., silicon, diamond, where n_0 is approximately the crystal bound electron density. For $L\sim 0.1$ cm, then $g_t=2\times10^{-4}$ cm^{-1} and low threshold values can be obtained in beam channeled DFB techniques. For the case the gain g is larger than the threshold gain g_t, the radiation fields $\epsilon_\pm$ increase with time as $\exp[(g-g_t)ct/2]$ in the linear range. Thus an amplification factor $(g-g_t)ct/2\sim 1$ is obtained for a beam pulse duration of 50 ns in $L=0.1$ cm for $g\sim 10$ cm^{-1}. This result should be compared to the gain $gL\sim 1$ obtained in a one passage amplification (with no reflections), wherefore $L=0.1$ cm, $g\sim 10$ cm^{-1}. In terms of beam current requirements the DFB mechanism in beam channeling has possible application in reducing current requirements by many orders of magnitude.

In the present treatment we have neglected radiation losses ($g_{\rm loss}$). It is possible making use of Borman anomalous transmission[13-16] that x-ray losses can be negligibly small. In an actual experiment the requirement of the Bragg condition would generate standing waves with nodes on the atomic sites, so that the condition for the Borman effect is fulfilled. Threshold conditions of the combined effects of the DFB mechanism and the Borman effect require further study.

The authors acknowledge useful discussions with Professor Amnon Fisher.

[1] J. U. Andersen, E. Bonderup, and R. H. Pantell, Ann. Rev. Nucl. Part. Sci. 33, 453 (1983).
[2] V. V. Beloshitsky and F. F. Komarov, Phys. Rep. 93, 117 (1982).
[3] G. Kurizki and J. K. McIver, Phys. Rev. B 32, 4358 (1985).
[4] R. K. Klein, J. O. Kephart, R. H. Pantell, H. Park, B. L. Berman, R. L. Swent, S. Datz, and R. W. Fearick, Phys. Rev. B 31, 68 (1985).

[8]B. L. Berman, B. A. Dahling, S. Datz, J. O. Kephart, R. K. Klein, R. H. Pantell, and H. Park, Nucl. Instrum. Methods B **10/11**, 611 (1985).
[9]V. V. Beloshitsky and M. A. Kumakhov, Phys. Lett. A **69**, 247 (1978).
[10]G. Kurizki, M. Strauss, J. Oreg, and N. Rostoker, Phys. Rev. A **35**, 3424 (1987).
[11]Y. H. Ohtsuki, Nucl. Instrum. Methods B **2**, 80 (1984).
[12]H. Kogelnik and C. V. Shank, Appl. Phys. Lett. **18**, 152 (1971); J. Appl. Phys. **43**, 2327 (1972).
[13]A. Yariv, Appl. Phys. Lett. **25**, 105 (1974).
[14]R. A. Fisher, Appl. Phys. Lett. **24**, 598 (1974).
[15]M. Strauss, P. Amendt, H. U. Rahman, and N. Rostoker, Phys. Rev. Lett. **55**, 406 (1985).
[16]B. W. Batterman, Rev. Mod. Phys. **36**, 681 (1964).
[17]B. Borie, Acta Crystallogr. **21**, 470 (1966).
[18]E. J. Saccocio and A. Zajac, Phys. Rev. **139**, 225 (1965).
[19]J. P. Hannon and G. T. Trammell, Opt. Commun. **15**, 330 (1975).

VIEWGRAPHS

CHANNELING X-RAY LASER

M. Strauss and N. Rostoker

Department of Physics

University of California

Irvine, California 92717

May 1989

X-RAY LASER CONCEPT

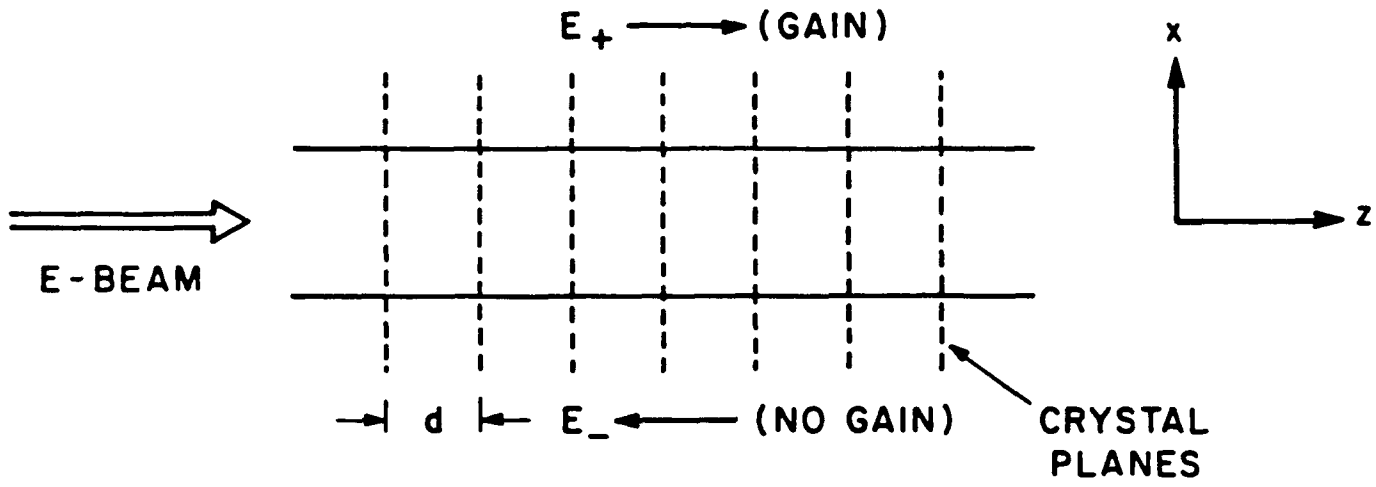

$\hbar\omega = 2\gamma^2\hbar\omega_0$ (DOPPLER) $\quad \lambda = 2d$ (BRAGG)

$= \hbar(\pi c/d)$ $\quad = 4A^\circ$

$d = 2 \times 10^{-8}$ cm $\quad \hbar\omega = 3$ keV (LiF CRYSTAL)

$\hbar\omega_0 = 4$eV $\quad (\gamma - 1)mc^2 = 9.2$ MeV

THEORETICAL PROBLEMS

COHERENCE LENGTH

SCATTERING PROCESSES

PHONONS, PLASMONS, IMPURITIES

POPULATION INVERSION

CAPTURE PROCESSES

PHONONS, ELECTRONS, SURFACE

GAIN CALCULATION

BRAGG REFLECTION / PHONONS

BORRMANN EFFECT

VIEWGRAPH 1

A. X-Ray Laser Concept

An efficient scheme to significantly reduce the gain requirements for a channeling X-ray laser is proposed. The scheme is based on the concept of a distributed feedback laser (DFB) induced by multiple Bragg reflections of the radiation.

A relativistic electron beam propagating through planar or axial crystal channels (z-direction) may populate transverse energy eigenstate due to the crystal transverse potential. Dipolar transitions between these discrete bound states ($\hbar\omega_o \sim$ 4 eV) yield narrow-width, highly polarized and intense Doppler up-shifted X-ray radiation ($\omega \sim 2\gamma^2 \omega_o$), which is strongly forward peaked. By adjusting the beam electron energy the emitted radiation can be tuned so that it satisfies the Bragg reflection condition for a set of planes in the transverse x-direction. The first order Bragg reflection is for $\lambda \simeq 2d$, where d is the periodic reflection plane spacing. A standing wave is generated by the forward amplified radiation field E_+ and the backward Bragg reflected field E_-.

This scheme has the advantages of a high degree of spectral selectivity with low gain per pass and without the need for cavity mirrors.

B. Theoretical Problems

The possibility of using the channeling mechanism as a coherent X-ray source depends on progress in the following areas:

(i) Increasing the coherence length for the channeling

particles. This length depends on the various scattering processes in the crystal such as phonons, plasmons and impurities.

(ii) Achieving significant population inversion. The inversion depends on the capture processes of the beam electrons from a free state to a bound state close to the crystal surface, and is affected by the interaction with crystal excitations such as phonons and crystal electrons.

(iii) Creating sufficient gain from induced emission. To reduce the high current density requirement on the beam a low gain concept is used based on Bragg reflection coupling. Standing waves are generated with nodes on the atomic sites which reduce drastically the effects of radiation absorption and the effects of atomic thermal motion (phonons), similar to the Borrmann anomalous transmission effect.

CHANNELING RADIATION

BEAM PARTICLE

$$-\frac{\hbar^2}{2\gamma m_e}\frac{\partial^2}{\partial x^2}\psi_i(x) + V(x)\psi_i(x) = \epsilon_i \psi_i(x)$$

$$\gamma = 1/\left[1-(v/c)^2\right]^{1/2}$$

$$\beta = v/c$$

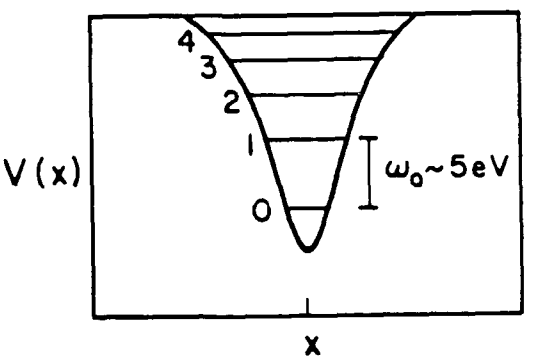

RADIATION

EMITTED PHOTON

$$\omega = \frac{\omega_0}{(1-\beta\cos\theta)} \simeq \frac{\omega_0}{1-\beta} \simeq 2\gamma^2\omega_0$$

DOPPLER SHIFT

$\theta \sim 0,\ \beta \sim 1$

$\omega_0 \sim 5eV$, $\gamma \sim 10-100$ $\longrightarrow$ $\omega \sim 1-100$ keV

SCALING LAWS

$$\gamma m_e \ddot{x} = -kx \longrightarrow \omega_0^2 = \frac{k}{\gamma m_e} \longrightarrow \omega_0 \sim \frac{1}{\gamma^{1/2}}$$

$$\omega \sim \gamma^{3/2}$$

VIEWGRAPH 2

CHANNELING RADIATION

A. Beam Particle

A channeling electron with energy in the range 5-100 MeV is attracted by the average planar potential V(x) and its transverse motion is non-relativistic. A set of discrete bound states are obtained by solving the Schroedinger equation, where the mass of the electron m is replaced by γm. The energy separation of the bound states, ω_o, is of the order of several eV. The planar potential depth is in the range 20-100 eV and several bound states can be found in the potential well. The channeling electron behaves as a bound particle in the transverse direction and relativistic free particle in the longitudinal direction.

B. Radiation

The radiation emitted by the bound channeling electron is mainly in the forward direction and as in a FEL it is Doppler upshifted, $\omega \simeq 2\gamma^2\omega_o$. Thus, for ω_o of several eV and γ ~ 10-100 the emitted radiation is in the X-ray range.

C. Scaling Laws

To obtain simple scaling laws we consider the case where the planar potential is of harmonic oscillator type and the channeling electron mass is γm. The oscillatory frequency $\omega_o \sim \gamma^{-1/2}$ and represents the energy separation of the bound channeling states. As γ increases ω_o decreases and more bound states can be included

in the potential well. The photon energy scales as $\omega \sim \gamma^{3/2}$ and increases with γ. The emitted photon energy depends on the particle energy γ and can be tuned close to Bragg reflection condition and a mirror-like structure is induced for the emitted radiation.

POPULATION INVERSION

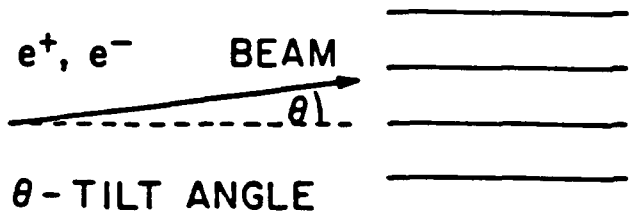

P.R. LETT. 49, 474, 1982

$$\left.\begin{array}{l}\text{(Transverse Energy) } \epsilon_\perp \sim 10\ \text{eV} \\ \text{(Beam Energy) } \epsilon_0 \sim 10\ \text{MeV}\end{array}\right\} \theta \sim \sqrt{\frac{\epsilon_\perp}{\epsilon_0}} = 1\ \text{mr}$$

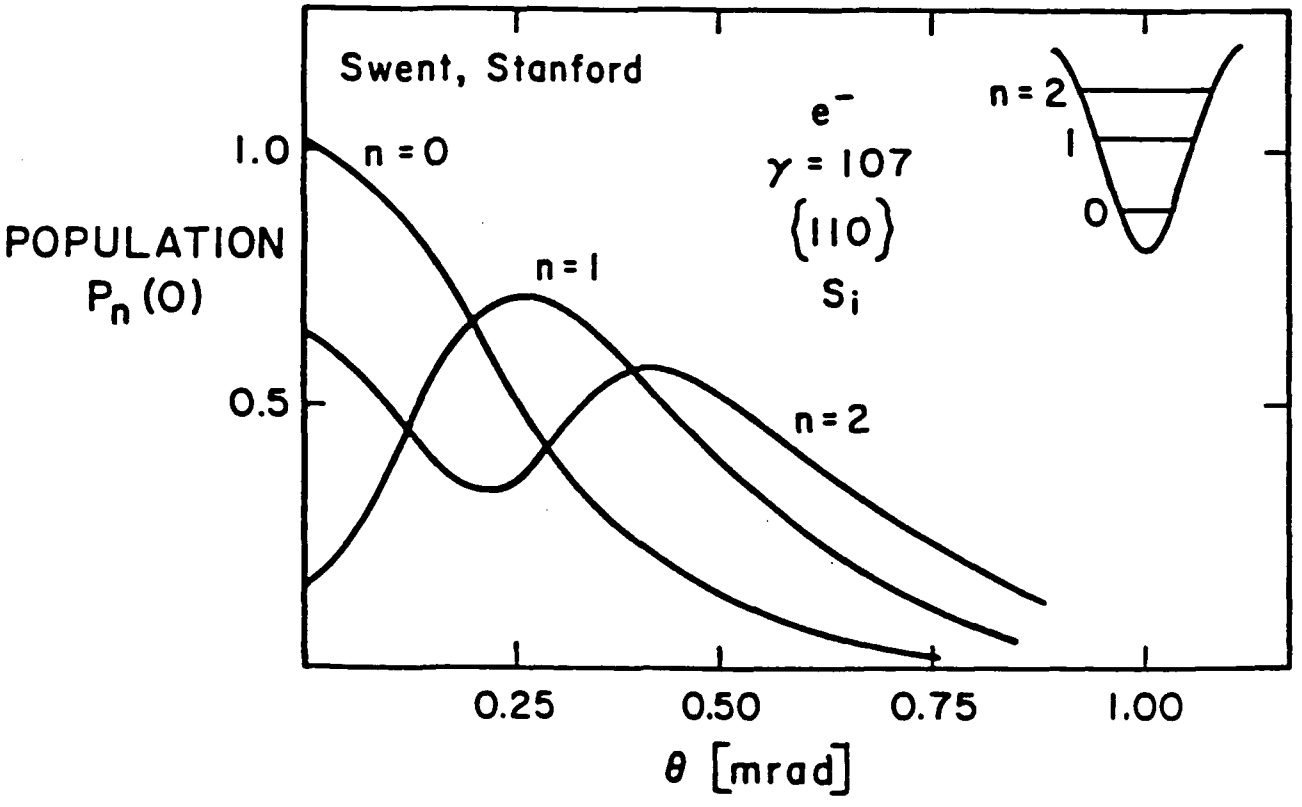

VIEWGRAPH 3

POPULATION INVERSION

A. Tilt Angle Scheme

By tilting the electron beam relative to a set of channeling atomic planes the particle acquires a transverse kinetic energy, and is more likely to be captured in higher bound states. This transverse energy should be smaller than the depth of the potential well. Thus, for a transverse energy of 10 eV and a channeling energy of 10 MeV the tilt angle should be of the order of 1 mrd. This range of tilt angles were obtained experimentally.

In the graph we see the population of three bound states (in arbitrary units) as a function of tilt angle. As the tilt angle increases the population of the lower state n=0 decreases and the population of state n=1 increases, so inversion is attained.

B. Recombination Scheme

This scheme is based on tilting the beam at relatively larger angles so that free states slightly above the potential well are populated. The process is equivalent to ionizing the channel. We can consider a recombination scheme where slightly free channeling particles interact with degenerate crystal electrons and are captured preferentially by higher bound states and generate population inversion. This scheme will be considered in future work.

CHANNEL RADIATION GAIN

$$g = \frac{2\pi\omega d^2 n_b W}{\hbar c \Gamma}\left[1 - \frac{v}{c}\right]^2$$

$$d = e\langle 1|x|2\rangle \qquad W = \rho_{22} - \rho_{11} \sim 1$$

$$\omega = 2\gamma^2\omega_o$$

$$g = \frac{e^2}{\hbar c}\,\frac{\pi}{\gamma^2}\,\frac{\omega_o}{\Gamma}\,\langle x\rangle^2\, n_b \cong 10^{-15}\, n_b$$

$$\omega_o = 6 \times 10^{15}\,\text{sec}^{-1}\ (4\text{eV})$$

$$\frac{c}{\Gamma} = 10^{-1}\,\text{cm} \qquad \langle x\rangle \sim 2\text{A}^\circ$$

$$\gamma = 21$$

$g = 10\,\text{cm}^{-1}$ $\qquad n_b = 10^{16}\,\text{cm}^{-3}$ $\qquad (4 \times 10^7\,\text{A/cm}^2)$

$g = 10^{-3}\,\text{cm}^{-1}$ $\qquad n_b = 10^{12}\,\text{cm}^{-3}$ $\qquad (4 \times 10^3\,\text{A/cm}^2)$

VIEWGRAPH 4

CHANNELING RADIATION GAIN

We would like to show that a channeling X-ray laser based on a single amplification pass would require a very high beam current density. Thus, the only practical scheme is to work in a low gain regime based on a mirror-like structure induced by Bragg reflections.

In a single pass laser we should attain $gL > 1$, where g is the gain factor and L is the amplification length. Here g is proportional to: the population inversion W (per channeling electron), the beam density n_b, the square of the dipole moment $d = e\langle x \rangle$, and the channeling coherence length c/Γ. For the following values: $L = 0.1$ cm, $g = 10$ cm^{-1}, $\omega_o \sim 4$ eV, $c/\Gamma = 0.1$ cm, $\langle x \rangle = 2$Å, $\gamma = 21$, $W \sim 1$ the required beam density is of the order 10^{16} cm^{-3} or a very high current density of 4×10^7 A/cm^2. We thus propose to apply the Bragg reflection multi-pass scheme, where the threshold gain can be reduced to the range $10^{-2} - 10^{-3}$ cm^{-1}, and the required current density can be of the order $10^4 - 10^5$ A/cm^2.

DISTRIBUTED FEEDBACK X-RAY LASER

$$g = \frac{2\pi\omega d^2 n_b W}{\hbar c \Gamma}(1-v/c)^2$$

$$\epsilon_+ = \epsilon_+(z) e^{(g-a)ct/2}$$

$$\alpha \equiv \frac{6}{k^2 L^3}$$

$$K = \frac{\pi n_b e^2}{mc\omega_B} \sim 5\times10^3 \text{ cm}^{-1}$$

$L \equiv 0.1$ cm

$\alpha = g_+ = 2.4\times10^{-4}\text{cm}^{-1}$ threshold gain

without reflections $gL \sim 1$ requires

$g \sim 10 \text{ cm}^{-1}$

with reflections and $t = 50$ nsec

$(g-\alpha)ct/2 \sim 1$ when $g \sim 10^{-3}\text{ cm}^{-1}$.

VIEWGRAPH 5

DISTRIBUTED FEEDBACK X-RAY LASER

By applying the Bragg reflection scheme the radiation field increases with time t as $\exp[(g-\alpha)ct/2]$ in the linear range, where α is the threshold gain factor. Here α depends on the losses in the system and for only reflection losses $\alpha = 6/K^2L^3$, where K is the reflection coefficient and L is the system length. For L = 0.1 cm and $K = 5 \times 10^3$ cm^{-1} the threshold gain $\alpha = 2.4 \times 10^{-4}$ cm^{-1} and is very small. An amplification factor $(g-\alpha)ct/2 \sim 1$ is obtained in a beam pulse duration t = 50 ns in L = 0.1 cm for $g \sim 10^{-3}$ cm^{-1}. This result should be compared to the gain $gL \sim 1$ obtained in a one passage amplification (with no reflections), where L = 0.1 cm, $g \sim 10$ cm^{-1}. In terms of beam current requirements the Bragg reflection scheme has possible application in reducing current density requirement by many orders of magnitude.

BORRMANN ANOMALOUS TRANSMISSION

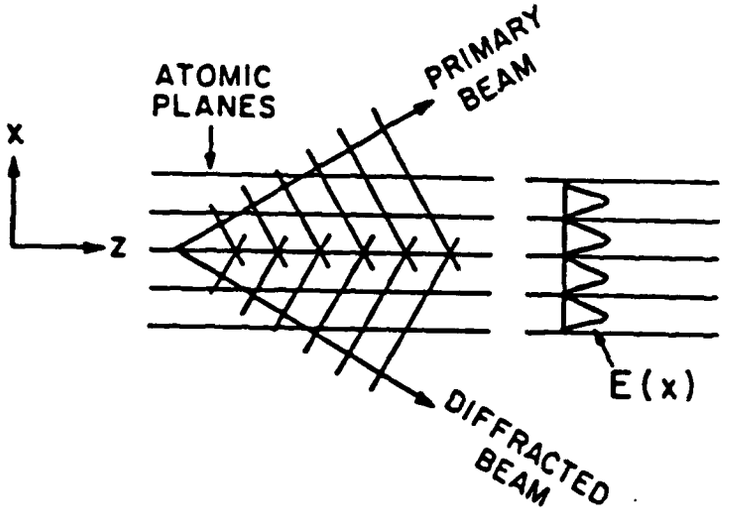

2-BEAM CASE
($\mu/\mu_0 \sim 10^{-3}$)

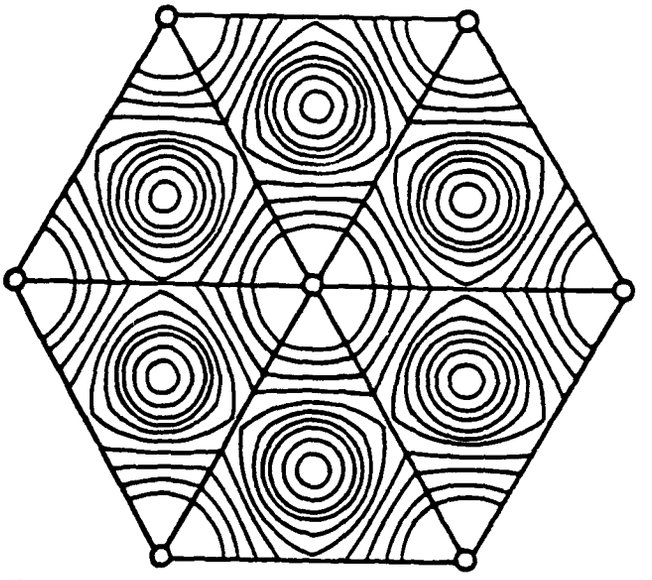

6-BEAM CASE
($\mu/\mu_0 \sim 10^{-4}$)

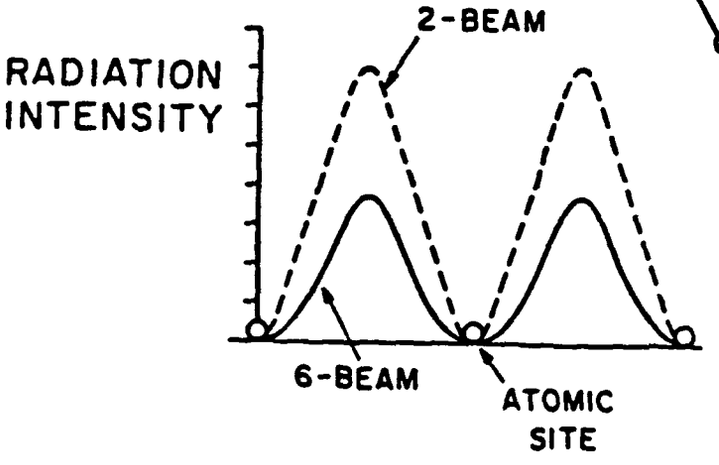

VIEWGRAPH 6

BORRMANN ANOMALOUS TRANSMISSION

In a channeling X-ray laser induced by Bragg reflections we should consider the absorption of the radiation by atomic bound electrons located close to the atomic sites. This loss mechanism can be drastically reduced by applying the Borrmann anomalous transmission effect.

A. Two-Beam Case

The Borrmann effect is obtained when a primary X-ray beam is Bragg reflected by a set of atomic planes. The primary and the diffracted beams, so called two-beam case, interfere to produce a standing wave perpendicular to the planes (x-direction) and a propagating wave parallel to the planes (z-direction). The nodes of the radiation are on the atomic sites which reduces drastically the radiation absorption. The absorption coefficient for the Borrmann mode μ relative to the average absorption μ_o can be reduced so that $\mu/\mu_o \sim 10^{-3}$.

B. Six-Beam Case

In order to further reduce the absorption losses of the radiation it is possible to consider diffraction from several sets of atomic planes which satisfy the Bragg condition simultaneously (dynamical diffraction theory). In the lower part of the viewgraph diffraction from three sets of atomic planes is shown (6-Beam Case). The radiation intensity contour has a larger nodal

region close to the atomic sites relative to the two-beam case and results in a further reduction in the radiation absorption. For this case the absorption coefficient for some of the radiation modes can be as small as $\mu/\mu_o \sim 10^{-4}$.

THRESHOLD GAIN CONDITION

LOSSES { ABSORPTION
ATOMIC MOTION

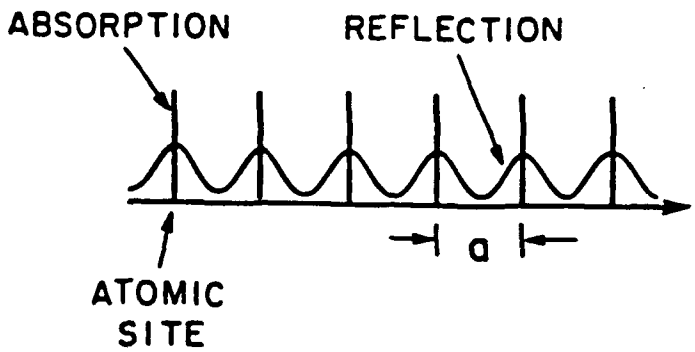

$$g_t = \frac{6e^{2Wn}}{K_n^2 L^3} + 2(\mu_o - e^{-Wn}\mu_n)$$

g_t ← THRESHOLD GAIN

n - ORDER OF BRAGG REFLECTION (Fourier Expansion)

$K_1 \sim 5 \times 10^3 cm^{-1}$ (Reflection)

$\mu_o \sim 10\ cm^{-1}$ (Average Absorption)

$1 - \mu_1/\mu_o \sim 10^{-3} cm^{-1}$ (Absorption)

$W_1 \sim 10^{-3}$ (Debye - Waller Factor, $T \ll T_D$)

$L \sim 0.1\ cm^{-1}$

$g_t \sim 10^{-2}\ cm^{-1}$

VIEWGRAPH 7

THRESHOLD GAIN CONDITION

The effects of radiation losses by absorption, including the thermal atomic motion, are presented for a channeling X-ray laser induced by Bragg reflection. Standing waves with nodes on the atomic sites are generated which reduces the radiation losses located close to the atomic sites. An explicit expression for the low-threshold gain g_t is presented which depends on the absorption, temperature and the order of Bragg reflections.

The first term in g_t is the effect of reflections, where K_n is the n order reflection coefficient and L is the system length. Here the thermal effects are included by a Debye-Waller factor W_n, which is very small for a temperature very low compared to the Debye temperature, $T << T_D$. The second term in g_t presents the effects of absorption, where μ_o and μ_n are the average and nth order absorption coefficients, respectively, and $\mu_o \sim \mu_n$. For the first order Bragg reflection and the values of K_1, μ_o, μ_1, W_1 and L presented in the viewgraph the threshold gain value can be as small as $g_t \sim 10^{-2}$ cm^{-1}. Thus Bragg reflection X-ray laser scheme has the possibility to reduce drastically radiation absorption.

RADIATION GUIDING IN BRAGG COUPLED X-RAY LASER

$\lambda = 3\text{Å}$

LOW CURRENT OPERATION	$I = 1\mu A - 1mA$
HIGH CURRENT DENSITY	$J = 10^4 - 10^5\ A/cm^2$
BEAM RADIUS	$a = 100\text{Å} - 1\mu m$

A) SPACE GUIDING

$$\frac{\lambda}{2a} < \frac{2a}{L} \longrightarrow F = 4a^2/\lambda L \gg 1$$

F: FRESNEL NUMBER

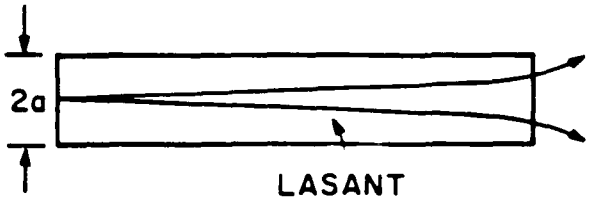

$L = 0.1\ cm$
$a = 1\mu m$
$g \ll 1\ cm^{-1}$
$\longrightarrow I \simeq 1mA$

B) REFLECTION OR ABSORPTION GUIDING

$$F = 4a/\lambda L_{eff} > 1 \quad , \quad 1/L_{eff} = \begin{cases} K_0 & \text{REFLECTION COEFFICIENT} \\ \mu_0 & \text{ABSORPTION COEFFICIENT} \end{cases}$$

$1/L_{eff}$: GUIDING MEDIUM

$1/L_{eff} = 10^4\ cm^{-1}$
$a = 100\ \text{Å}$
$g \ll 1\ cm^{-1}$
$\longrightarrow I \simeq 1\mu A$

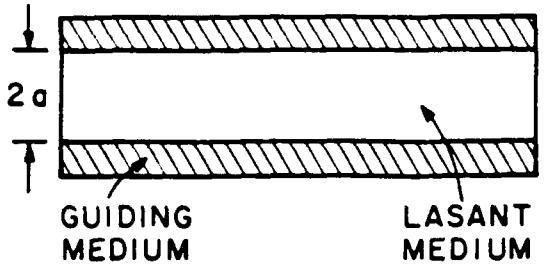

C) SUPER-LATTICE CRYSTAL AND MIXED GUIDING

$a_x = 100\text{Å}$ MEDIUM GUIDING
$a_y = 1\mu m$ SPACE GUIDING
$\longrightarrow I \simeq 10\mu A$

VIEWGRAPH 8

RADIATION GUIDING IN BRAGG COUPLED X-RAY LASER

In order to test the applicability of a Bragg reflection X-ray laser scheme we can consider a high current density electron beam (10^4 - 10^5 A/cm^2) with low emittance, but with very small total current (1 mA - 1 μA). Similar beams are used in scanning electron microscopy in DC operation. In such beams the radius can be in the range 100Å - 1 μm and radiation guiding to avoid diffraction out of the amplification medium is important. It is possible to consider gain guiding mechanism with $F = 4a^2g/\lambda > 1$, where g is the gain factor and a is the beam radius. But in our low gain scheme gain guiding cannot be maintained.

A. Space Guiding

Spatial diffraction of the radiation out of the lasant region can be avoided for Fresnel number $F = 4a^2/\lambda L >> 1$, where L is the system length. For L = 0.1 cm, λ = 3Å then a $\geq$ 1 μm and the total current must be I - 1 mA.

B. Reflection or Absorption Guiding

Radiation guiding can be maintained for a smaller beam radius by using a guiding medium in the transverse direction which surrounds the lasant medium. For this case the effective Fresnel number for guiding is $F = 4a^2/\lambda L_{eff} > 1$, where L_{eff} depends on the guiding material. Here L_{eff} can be $1/K_o$ for reflection guiding or $1/\mu_o$ for absorption guiding, where K_o and μ_o are the

average reflection or absorption coefficient of the guiding medium, respectively. For the case $1/L_{eff} = 10^4$ cm^{-1}, $\lambda = 3Å$ then $a \geq 100Å$ and the total current can be as small as 1 μA.

It is useful to consider mixed guiding conditions where guiding in one transverse direction is maintained by Fresnel spatial guiding and in the other transverse direction by a planar guiding medium. One can consider a super-lattice crystal with lasant channeling planar regions surrounded by guiding planar medium. For such a system radiation guiding can be maintained in a beam transverse dimension of (100Å) x (1 μm) and with a low beam current of 10 μA.

WIDE BEAM X-RAY LASER SCHEME

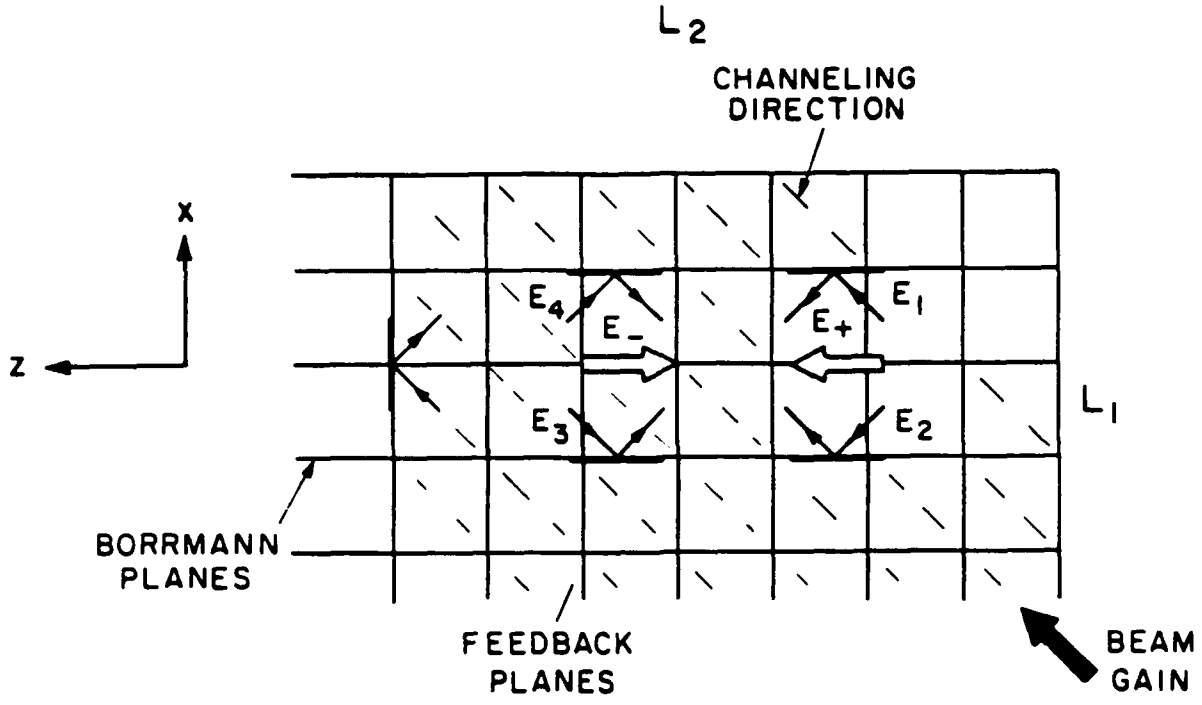

E_1 - GAIN

$L_1 \ll L_2$ { $L_1 \sim$ CHANNELING LENGTH ; $L_2 \sim$ BEAM DIMENSION

(+ Z Energy Flow) $E_+ = E_1 + E_2 = (e^{ik_x x} + e^{-ik_x x})\, e^{ik_z z}$

(- Z Energy Flow) $E_- = E_3 + E_4 = (e^{ik_x x} + e^{-ik_x x})\, e^{-ik_z z}$

$E = E_+ + E_-$ (Standing Waves in x and z Direction)

VIEWGRAPH 9

WIDE BEAM X-RAY LASER SCHEME

In some crystals the length the electron stays in the bound channeling state (the channeling length) may be shorter than the required amplification length. In this case the losses may increase the required threshold gain. In order to overcome this difficulty we propose a scheme which is independent of the channeling length. The scheme is based on directing the emitted radiation by Bragg reflections so that the amplification direction differs from the channeling direction. As we can see from the viewgraph the transverse dimension of the beam covers the lasant region L_2 in the amplification direction z. The channeling length L_1 defines the transverse dimension of the amplification medium and $L_1 << L_2$.

Radiation field E_1 is emitted by the beam and amplified in the channeling direction. Two sets of planes in the X and Z directions are used to reflect the radiation and to generate equal amplitude fields E_2, E_3 and E_4. A radiation mode is generated with $E_+ = E_1 + E_2$ and $E_- = E_3 + E_4$ which generates energy flow in the +Z and -Z directions, respectively. A standing wave is attained in the X and Z directions with nodes on the atomic sites to reduce absorption.

This scheme can be used for a beam of transverse dimensions of 0.1 cm in the Z direction and 100Å in the y direction, with a total current in the range 1-10 mA. It is possible to scale-up to larger X-ray lasers by increasing the transverse dimension of the beam independent of the channeling length.

ACCELERATORS

EMITTANCE $\epsilon = R\langle\Delta\theta\rangle$

NORMALIZED $\epsilon_N = \gamma\beta R\langle\Delta\theta\rangle = P_\perp R/C$

BRIGHTNESS $B = \frac{J}{\Delta\Omega} = \frac{I}{(\pi\epsilon)^2}$

FOCUSING – ENVELOPE EQUATION

$$\frac{d^2r}{dz^2} = \frac{\epsilon^2}{r^3} + \frac{2\nu}{\gamma r}\left[1 - f_e - \beta^2(1 - f_m)\right] - \frac{\Omega_z^2}{2c^2} r$$

EMITTANCE SELF FIELDS EXTERNAL FIELD

MAGNETIC LENS IN VACUUM

$$\frac{d^2r}{dz^2} = \frac{\epsilon^2}{r^3} + \frac{2\nu}{\gamma^3}\frac{1}{r} - \frac{\Omega_z^2}{2c^2} r$$

VIEWGRAPH 10

ACCELERATORS

Beam quality is expressed by emittance and brightness which are defined. The normalized emittance ϵ_N is useful because it does not change when acceleration takes place and can thus be used to determine the change in emittance ϵ (assuming there are no instabilities).

Focusing involves the emittance, a defocusing term, self fields which in a plasma can be either focusing or defocusing and the external focusing field of a magnetic lens. Focusing is described by the envelope equation. In vacuum the self fields are always defocusing and only this case will be further considered.

FOCUSING LIMITS

$$\langle \Delta\theta \rangle_F = \epsilon / R_m$$

$$\frac{\gamma m}{2} \left(c \langle \Delta\theta \rangle_F \right)^2 \leq W_\perp = 100\,\text{eV}$$

$$R_m = \epsilon \sqrt{\frac{\gamma mc^2}{2W_\perp}}$$

$$J_m = Bx \frac{2W_\perp}{\gamma mc^2}$$

VIEWGRAPH 11

FOCUSING LIMITS

The minimum radius is related to the angular spread of a beam through the emittance which is constant if focusing takes place, but no acceleration. Focusing the beam increases the perpendicular energy. If this is limited to $W_{\perp}$ = 100 eV, for example, so that electrons remain in a channel of maximum potential 100 eV, there is a minimum radius to which the beam can be focused and a maximum current density J_m, or electron beam density n_m.

ACCELERATOR COMPARISONS

	I AMP	ϵ R-cm	B A/cm^2 STR	γ	J_m A/cm^2	R_m cm	n_m cm^{-3}
ETA (LLNL) (50 nsec pulse)	10^4	5×10^{-3}	1.3×10^8	21	2.5×10^3	1	5×10^{11}
STELLATRON (UCI)	10^3	5×10^{-3}	1.3×10^7	21	250	1	5×10^{10}
LINAC-RF (LLNL)	2×10^{-2}	5×10^{-5}	2.5×10^6	21	50	10^{-2}	10^{10}
FIELD EMISSION* 5 keV - D.C.	10^{-8}	3×10^{-8}	1.1×10^6	1	0.32×10^6	10^{-7}	4.7×10^{14}
ACCELERATE TO 5 MeV	10^{-8}	3.8×10^{-10}	7×10^9	11	0.8×10^6	6.3×10^{-8}	1.7×10^{14}

* J.F. HAINFIELD IN SCANNING ELECTRON MICROSCOPY VOL I P591-604 (1977)

VIEWGRAPH 12

ACCELERATOR COMPARISONS

Various accelerators are compared on the basis of the value of J_m or n_m that can be achieved subject to the limitation of $W_\perp \leq 100$ eV. The field emission electron source used for a scanning electron microscope is by far the best source from this perspective. For $W_\perp = 10$ eV and a final γ of 21 the maximum current density would also be $.8 \times 10^6$ A/cm^2. The total current has been limited to 10^{-8} A-d.c. to avoid damage to the emitter. For pulsed operation much larger currents should be feasible without emitter damage.

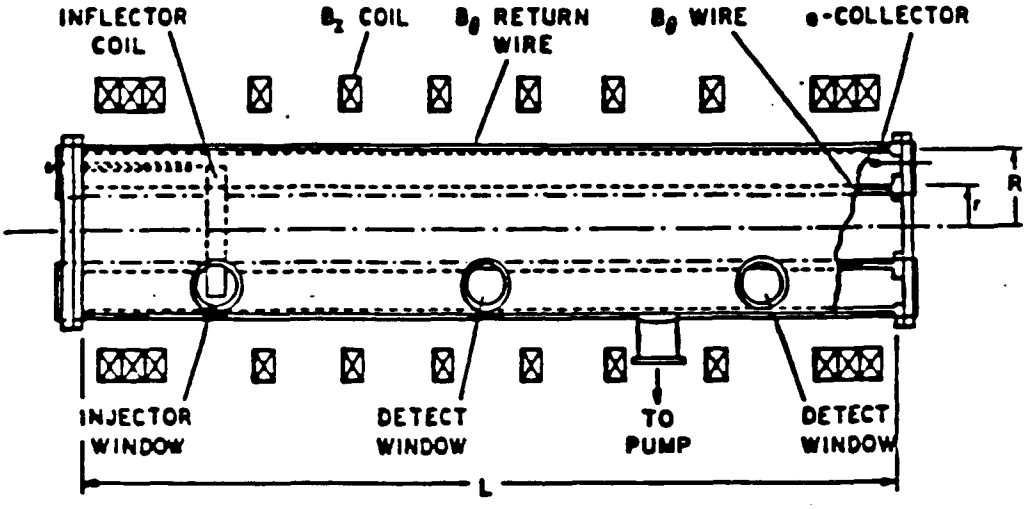

Vacuum Chamber and Coils

For the Elongated Betatron

VIEWGRAPH 13

ACCELERATOR DEVELOPMENT

If it is possible to accelerate a low current beam from 5 keV to 10 MeV without changing the normalized emittance, then it should be feasible to make a channel radiation X-ray laser with low threshold gain g ~ 10^{-2}/cm. The most obvious accelerator for this is a Van der Graf, but it is quite large and expensive. For low currents less than 1 milliampere there should be no problem with instabilities in a conventional Betatron. The problem is that it is quite difficult to trap a low current cold beam in a conventional Betatron. We therefore consider an elongated Betatron as illustrated in the viewgraph where this problem has been solved. Injection is greatly simplified because an electron must travel the length of the accelerator and be reflected back to the injector in order to be lost by striking the injector. Since the axial velocity can be as low as 1% of the velocity of light and the length between mirrors, 1 meter, the transit time before striking the injector would be 666 nsec. This is sufficient time to change the magnetic field with the reflector coil so that the beam would not reach the injector. The corresponding time for a conventional Betatron of radius 50 cm would be 10 nsec. Both trapping and acceleration have been accomplished with the elongated Betatron and with a low current collective instabilities should be absent. We are also re-examining the problem of trapping in a conventional Betatron because it seems to have been accomplished in Soviet experiments. (Institute of Optical and

Physical Measurements, Moscow, Drs. Panafjuk and Stepanov, as reported by Dr. F. Felber [1983]).

PUBLICATIONS IN CHANNELING RADIATION

1. M. Strauss, P. Amendt, H. U. Rahman and N. Rostoker, Phys. Rev. Lett. 55, 406 (1985), Line Shifts in Electron Channeling Radiation from Lattice Vibrations.
2. P. Amendt, M. Strauss, H. U. Rahman and N. Rostoker, Phys. Rev. A 33, 839 (1986), Valence-Band Plasmon Effects on Line Shifts and Widths in Positron Planar-Channeling Radiation.
3. G. Kurizki, M. Strauss, J. Oreg and N. Rostoker, Phys. Rev. A 35, 3424 (1987), Theory of Short-Wavelength Lasing from Channeled Projectiles: Nondegenerate Dipole Transitions.
4. M. Strauss, P. Amendt, N. Rostoker and A. Ron, Appl. Phys. Lett. 52, 866 (1988); IEEE Plasma Science 16, 548 (1988), X-Ray Laser Gain from Bragg Reflection Coupling in Channeled Relativistic Beam System.
5. M. Strauss, Phys. Rev. A 38, 1358 (1988), Buildup of X-Ray Laser Gain by Fluctuations in Channeled Relativistic Beam System.
6. M. Strauss and N. Rostoker, Phys. Rev. A 39, June (1989), Reduced Radiation Losses in a Channeled-Beam X-Ray Laser by Bragg Reflection Coupling.

PHYSICAL REVIEW A VOLUME 39, NUMBER 11 JUNE 1, 1989

Reduced radiation losses in a channeled-beam x-ray laser by Bragg reflection coupling

M. Strauss* and N. Rostoker
Department of Physics, University of California, Irvine, California 92717
(Received 19 December 1988)

The effects of radiation losses and atomic motion in a distributed feedback induced by Bragg reflections in an electron-beam-channeling x-ray laser are investigated. Standing-wave fields with nodes in the atomic sites are generated in this cavity-mirror structure in single crystals, thereby reducing the losses located close to the atomic sites. An explicit expression for the low-threshold gain is derived which depends on the absorption, temperature, and on the order of Bragg reflection. It is noted that diffraction from several sets of atomic planes which satisfy the Bragg condition simultaneously may further reduce the threshold gain. These distributed-feedback schemes have possible application in reducing beam high-current requirements by many orders of magnitude.

I. INTRODUCTION

A relativistic electron beam propagating through planar or axial channels in a crystal free of imperfections may populate bound transverse-energy eigenstates.[1] Spontaneous dipolar transitions between these discrete eigenstates have been shown experimentally to yield narrow-width, highly polarized, and intense x-ray radiation which is strongly forward peaked.[2] One of the important issues in the possibility of using the channeling mechanism as a coherent x-ray source depends on future progress in creating sufficient gain from induced emission. this paper is related to the issue of identifying an efficient scheme for gain optimization in crystal channeling. Previous estimates suggest that in a one-passage amplification scheme even modest gains may require currents of the order of MA/cm^2 for energies near 10 MeV.[3-5] The aim should be to suggest a mechanism to reduce this high-current requirement by many others of magnitude, thereby bringing one aspect of the channeling x-ray laser closer to experimental reach.

An efficient scheme to significantly reduce the gain requirements for a channeling x-ray laser was proposed based on the concept of a distributed-feedback (DFB) laser which is supplied by multiple Bragg reflections of the radiation.[6] This scheme was very useful for atomic emitters in the optical range[7] and was extended later on to the x-ray range.[8] The advantages in using DFB lasers include the intrinsic compactness and high degree of spectral selectivity available without the need for cavity mirrors. The channeling DFB concept is favorable due to the possibility of radiation tunability. By adjusting the electron-beam energy the Doppler up-shifted radiation can be tuned onto a line in the DFB-mode spectrum near the Bragg-reflection frequency.[6] In Ref. 6 the threshold-gain condition for a DFB x-ray laser was obtained taking into account only reflections and neglecting the radiation losses in the crystal. The main loss mechanism is the photoelectric absorption by tightly bound electrons located close to the atomic sites in the crystal. Furthermore, the atomic motion in the crystal was ignored, which may influence the absorption and the reflections of the radiation.

This paper considers the channeling DFB scheme including the effects of absorption and atomic motion on the threshold-gain condition and spectral selectivity. We find that the formation of a standing-wave field with nodes on atomic sites, where absorption takes place, reduces drastically the effect of absorption. This effect is related to the Borrmann anomalous-transmission effect where standing-wave generation makes x-ray losses small.[9-12] The effects of atomic motion on increasing absorption and reducing reflections are considered. This effect is due to the zero-point motion at low temperatures and due to the thermal motion at higher temperatures relative to the Debye temperature. The atomic-motion effect can be expressed in terms of a Debye-Waller factor.[10,13,14] This effect limits the applicability of the DFB scheme to temperatures that are very low compared to the Debye temperature. We further consider the effect of the order of Bragg reflections on the threshold-gain condition. In spite of the limitations introduced by the radiation losses the DFB mechanism does reduce drastically the high-current requirements. However, the main threshold condition is dictated by the absorption.

It is pointed out that it is possible to further reduce the threshold gain by diffraction from several sets of atomic planes which satisfy the Bragg condition simultaneously.[15,16] In this case standing waves are generated in several directions relative to an atomic site, generating a larger nodal region in the radiation field and reducing the effects of radiation losses.

In Sec. II we present the DFB x-ray laser model including absorption but neglecting the atomic motion in the crystal. The inclusion of atomic motion is considered in Sec. III. In Sec. IV we obtained the threshold and selectivity conditions. Numerical results and discussion are presented in Sec. V.

II. THE DFB X-RAY LASER MODEL

We characterize the set of channeling transverse eigenstates in the x direction as a two-level system with states

$|1\rangle$ and $|2\rangle$, where W and $\hbar\omega_0=\varepsilon_2-\varepsilon_1$ are the population and energy differences, respectively. The directions of beam channeling and Bragg reflections are taken in the z direction. The Doppler up-shifted electromagnetic wave frequency $\omega=\omega_0/(1-v/c)\simeq 2\gamma^2\omega_0$ in the forward direction is chosen to closely match the n-order Bragg frequency, $\omega\sim n\omega_B$, where v is the channeling-electron speed, $\omega_B=\pi c/a$ and a is the the periodic reflection-plane spacing. Typically $\hbar\omega_0$ is a few electron volts in the laboratory frame so that for the relativistic factor γ on the order of 20, $\hbar\omega$ is on the order of several keV. Consequently, the channeling-electron energy may be tuned to satisfy the Bragg-reflection condition and induce distributed feedback in the channeling crystal.

The behavior of the electric $\mathbf{E}$ field of the electromagnetic wave and the polarization $\mathbf{P}$ of the beam electrons are related by the Maxwell's wave equation:

$$\frac{\partial^2}{\partial z^2}\mathbf{E}-\frac{1}{c^2}\frac{\partial^2}{\partial t^2}\mathbf{E}=\frac{4\pi}{c^2}\frac{\partial}{\partial t}\left[\frac{\partial}{\partial t}\mathbf{P}+c\nabla\times\mathbf{M}+\mathbf{J}\right], \quad (1)$$

where $\mathbf{M}=\mathbf{P}\times\mathbf{v}/c$ is the magnetization due to the beam electrons and transverse-field effects are not considered.[4] The induced current $\mathbf{J}=\mathbf{J}_{osc}+\mathbf{J}_{los}$, where $\mathbf{J}_{osc}$ is the oscillatory part and $\mathbf{J}_{los}$ is the dissipative current. We approximate $\mathbf{J}_{osc}=n_e e\mathbf{v}_e$ and $(\partial/\partial t)\mathbf{J}_{osc}=e^2 n_e\mathbf{E}/m_e$, where n_e is the spatially modulated atomic-electron density.[6,8] The current $\mathbf{J}_{osc}$ provides coupling between the forward- and backward-propagating waves and is mainly due to the outer cloud of atomic electrons. The current $\mathbf{J}_{los}=\sigma\mathbf{E}$, where σ is the modulated dissipative conductivity, and represents the photoelectric absorption of the radiation by the tightly bound electrons close to the atomic sites.[10] The induced current $\mathbf{J}$ in the right-hand side of Eq. (1) can be represented as

$$\frac{\partial}{\partial t}\mathbf{J}=\frac{c}{2\pi}\left[\omega K\mathbf{E}+\mu\frac{\partial\mathbf{E}}{\partial t}\right], \quad (2)$$

where $K=2\pi e^2 n_e/cm\omega$ is the reflection function, $\mu=2\pi\sigma/c$ is the absorption function, and an average is carried out over the transverse direction $\rho=(x,y)$. In this section the atomic motion is neglected so that K and μ are periodic functions in the z direction.

The electric $\mathbf{E}$ and polarization $\mathbf{P}$ fields are taken in the x direction and are defined in term of forward- and backward-traveling waves,

$$E(z,t)=\varepsilon_+(z,t)e^{-i(\omega t-z/c)}+\varepsilon_-(z,t)e^{-i(\omega t+z/c)}+\text{c.c.}, \quad (3a)$$

$$P(z,t)=P_+(z,t)e^{-i(\omega t-z/c)}+P_-(z,t)e^{-i(\omega t+z/c)}+\text{c.c.}, \quad (3b)$$

where $\varepsilon_\pm$ and $P_\pm$ are slowly varying envelope fields. Inserting Eqs. (3a), (3b), and (2) in Eq. (1) we obtain

$$e^{ikz}\left[\frac{\partial\varepsilon_+}{\partial z}+\frac{1}{c}\frac{\partial\varepsilon_+}{\partial t}+(\mu+iK)\varepsilon_+\right]+e^{-ikz}\left[-\frac{\partial\varepsilon_-}{\partial z}+\frac{1}{c}\frac{\partial\varepsilon_-}{\partial t}+(\mu+iK)\varepsilon_-\right]=\frac{2\pi i\omega}{c}[e^{ikz}(1-v/c)P_+ +e^{-ikz}(1+v/c)P_-], \quad (4)$$

where $k=\omega/c$ and second-order derivatives are ignored because $\partial^2\varepsilon_\pm/\partial t^2\ll\omega\partial\varepsilon/\partial t$ and $\partial^2\varepsilon_\pm/\partial z^2\ll k\partial\varepsilon/\partial z$.

Equation (4) must be supplemented by the equation for $P_\pm$ and is readily determined from a density-matrix approach obeying the Bloch equation[4,17]

$$\frac{\partial}{\partial t}P_\pm+v\frac{\partial}{\partial z}P_\pm=i\Delta_\pm P_\pm-i(1\mp v/c)d^2 n_b W\varepsilon_\pm/\hbar-\Gamma P_\pm, \quad (5)$$

where $d=e\langle 1|x|2\rangle$ is the electric dipole moment, n_b is the beam number density, Γ is the phenomenological damping constant related to the channeling coherence length v/Γ, $\Delta_\pm=\omega(1\mp v/c)-\omega_0$ is a detuning frequency, and v/c represents a magnetic dipole interaction correction. In the limit of short coherence v/Γ the left-hand side of Eq. (5) is small and Eq. (5) simplifies

$$P_\pm\simeq id n_b W(d\varepsilon_\pm/\hbar)(1\mp v/c)/(i\Delta_\pm-\Gamma).$$

Near resonance $\omega\sim 2\gamma^2\omega_0$ and $\Delta_+/\Gamma\ll 1$ giving

$$P_+=-id^2 n_b W\varepsilon_+(1-v/c)/\hbar\Gamma. \quad (6)$$

In this limit $\Delta_-\sim\omega$, $\Delta_-\gg\Gamma$, and in the case of low gain, P_- can be ignored in Eq. (4). We now define the scalar gain $g=2\pi\omega(d_1)^2 n_b W/\hbar c\Gamma$, where $d_1=d(1-v/c)$. Substituting Eq. (6) in Eq. (4) we obtain

$$e^{ikz}\left[\frac{\partial}{\partial z}\varepsilon_+ +\frac{1}{c}\frac{\partial}{\partial t}\varepsilon_+ +(\mu+iK)\varepsilon_+ -g_+\varepsilon_+\right]+e^{-ikz}\left[-\frac{\partial}{\partial z}\varepsilon_- +\frac{1}{c}\frac{\partial}{\partial t}\varepsilon_- +(\mu+iK)\varepsilon_- -g_-\varepsilon_-\right]=0, \quad (7)$$

where the forward gain factor $g_+=g$ and the backward gain factor $g_-=0$.

In the following we obtain the equation of motion for DFB x-ray laser by using the resonance parts of Eq. (7). Notice that K and μ are the periodic functions, i.e., $K(z)=K(z+a)$ and $\mu(z)=\mu(z+a)$. For a periodic function $f(z)=f(z+a)$ we can use the Fourier-series expansion

$$f(z)=\sum_{l=-\infty}^{\infty}f_l e^{2ilk_B z}, \quad (8)$$

where $k_B=\omega_B/c=\pi/a$ and

$$f_l=\frac{1}{a}\int_{-a/2}^{a/2}dz\, f(z)e^{-2ilk_Bz}\ . \tag{9}$$

We insert the Fourier expansion Eq. (8) for K and μ in Eq. (7). For the case the radiation frequency is close to the n-order Bragg-reflection condition $k\sim nk_B$ and ignoring highly oscillatory terms we obtain from Eq. (7)

$$\frac{\partial}{\partial z}\varepsilon_+ +\frac{1}{c}\frac{\partial\varepsilon_+}{\partial t}+(\mu_0+iK_0)\varepsilon_+ +(\mu_n+iK_n)\varepsilon_-e^{-2i(k-nk_B)z}=g_+\varepsilon_+\ , \tag{10}$$

$$-\frac{\partial}{\partial z}\varepsilon_- +\frac{1}{c}\frac{\partial\varepsilon_-}{\partial t}+(\mu_0+iK_0)\varepsilon_- +(\mu_{-n}+iK_{-n})\varepsilon_+e^{2i(k-nk_B)z}=g_-\varepsilon_-\ , \tag{11}$$

where to obtain Eq. (10) and Eq. (11) we divide Eq. (7) by $\exp(ikz)$ and $\exp(-ikz)$, respectively, and keep only the resonance terms. Finally we redefine $\varepsilon_\pm$ as $\varepsilon_\pm\exp[\mp i(k-nk_B)z]$ and get

$$\frac{\partial}{\partial z}\varepsilon_+ +\frac{1}{c}\frac{\partial\varepsilon_+}{\partial t}-(g_+-i\delta-\mu_0-iK_0)\varepsilon_+ +(\mu_n+iK_n)\varepsilon_-=0\ , \tag{12}$$

$$-\frac{\partial}{\partial z}\varepsilon_- +\frac{1}{c}\frac{\partial\varepsilon_-}{\partial t}-(g_--i\delta-\mu_0-iK_0)\varepsilon_- +(\mu_n^*+iK_n^*)\varepsilon_+=0\ , \tag{13}$$

where $\delta=nk_B-k$ is the detuning from the n-order Bragg reflection. We have assumed that K and μ are real functions, i.e., $K_{-m}=K_m^*$ and $\mu_{-m}=\mu_m^*$. Equations (12) and (13) are a coupled set of equations of motion for the DFB x-ray laser. In Sec. III we include the average effect of the atomic motion in the crystal on Eqs. (12) and (13).

III. ATOMIC MOTION EFFECTS ON THE DFB EQUATIONS

To include the atomic motion effects in an approximate manner we introduce the reflection function K and absorption function μ as an ensemble average over a set of realizations of atomic displacements,

$$K(z)=\langle\hat{K}(z)\rangle,\quad \mu(z)=\langle\hat{\mu}(z)\rangle\ ,$$

where $\hat{K}(z)$ and $\hat{\mu}(z)$ are the reflection and absorption functions, respectively, for a given realization averaged over the transverse direction ρ. To carry out the averaging procedure on $\hat{K}$ and $\hat{\mu}$ we consider a general function $f(z)$ such that $f(z)=\langle\hat{f}(z)\rangle$, where $f(z)$ is a periodic function $f(z)=f(z+a)$. We can write $\hat{f}$ as

$$\hat{f}(z)=\sum_j\{V(\mathbf{r}-\mathbf{R}_j-\mathbf{U}_j)\}_\perp\ , \tag{14}$$

where $V(\mathbf{r}-\mathbf{R}_j-\mathbf{U}_j)$ is the contribution at $\mathbf{r}=(\rho,z)$ of the atom located close to site $\mathbf{R}_j$ with an atomic displacement $\mathbf{U}_j$. Here $\{V\}_\perp$ is an average over the transverse direction. Applying a Fourier-series expansion and averaging over the transverse direction we obtain

$$\hat{f}(z)=\sum_j\sum_{k_z}V(k_z)e^{ik_z(z-R_j^{(z)}-U_j^{(z)})}\ , \tag{15}$$

where $R_j^{(z)}$ and $U_j^{(z)}$ are the z components of $\mathbf{R}_j$ and $\mathbf{U}_j$, respectively. Here k_z is the z component of the Fourier-series expansion.

In order to find the ensemble average of $\hat{f}$ we use the average relation for a harmonic crystal[18]

$$\langle e^{ik_zU_j^{(z)}}\rangle=\exp[-k_z^2\langle(U_j^{(z)})^2\rangle/2] \tag{16}$$

and obtain

$$f(z)=\sum_j\sum_{l=-\infty}^{\infty}V(k_l)e^{-k_l^2\langle(U_j^{(z)})^2\rangle/2}e^{ik_l(z-R_j^{(z)})}\ , \tag{17}$$

where in Eq. (17) we use the fact that for $f(z)$ periodic the only contribution is for $k_z=k_l\equiv 2lk_B$ and l is an integer.

To find the ensemble average $\langle(U_j^{(z)})^2\rangle$ we use the phonon representation for $\mathbf{U}_j$. For simplicity we consider a monatomic crystal of atomic mass M and with N unit cells,[18]

$$\mathbf{U}_j=\frac{1}{\sqrt{N}}\sum_{\mathbf{q},s}\left[\frac{\hbar}{2M\omega_{\mathbf{q}s}}\right]^{1/2}(C_{\mathbf{q}s}+C_{-\mathbf{q}s})\boldsymbol{\epsilon}_s(\mathbf{q})e^{i\mathbf{q}\cdot\mathbf{R}_j}\ , \tag{18}$$

where $C_{\mathbf{q}s}$ ($C_{\mathbf{q}s}^\dagger$) is the creation (annihilation) operator of a phonon with momentum $\mathbf{q}$, frequency $\omega_{\mathbf{q}s}$, polarization vector $\boldsymbol{\epsilon}_s(\mathbf{q})$, and $\boldsymbol{\epsilon}_s(\mathbf{q})=\boldsymbol{\epsilon}_s^*(-\mathbf{q})$. The sum s in Eq. (18) is over all the possible phonons bands. Using the ensemble-average relations

$$\langle C_{\mathbf{q}s}^\dagger C_{\mathbf{q}s}\rangle=n_{\mathbf{q}s},\quad \langle C_{\mathbf{q}s}C_{\mathbf{q}s}^\dagger\rangle=n_{\mathbf{q}s}+1,\quad \langle C_{\mathbf{q}s}C_{\mathbf{q}s}\rangle=0\ ,$$

where $n_{\mathbf{q}s}$ is the occupation number of the phonon $\mathbf{q}s$ and depend on the temperature of the system, we obtain

$$\langle(U_j^{(z)})^2\rangle=\frac{1}{N}\sum_{\mathbf{q},s}\left[\frac{\hbar}{2M\omega_{\mathbf{q}s}}\right](2n_{\mathbf{q}s}+1)[\boldsymbol{\epsilon}_s(\mathbf{q})\cdot\hat{\mathbf{z}}]^2\ . \tag{19}$$

Equation (19) is independent of the specific location j.

We define the Debye-Waller factor[18] as $W_l=k_l^2\langle(U_j^{(z)})^2\rangle/2$ and use Eq. (19) to obtain

$$W_l=\frac{2(lk_B)^2}{N}\sum_{\mathbf{q},s}\left[\frac{\hbar}{2M\omega_{\mathbf{q}s}}\right](2n_{\mathbf{q}s}+1)[\boldsymbol{\epsilon}_s(\mathbf{q})\cdot\hat{\mathbf{z}}]^2\ . \tag{20}$$

From Eqs. (19) and (20) we can rewrite Eq. (17) as a series expansion,

$$f(z)=\sum_{l=-\infty}^{\infty}(f_le^{-W_l})e^{2ilk_Bz}\ , \tag{21}$$

where

$$f_l=\sum_j V(2lk_B)e^{-2ilk_BR_j^{(z)}}\ .$$

Comparing Eqs. (21) and (8) we find that the inclusion of the atomic motion is by replacing f_l by a Debye-Waller-dependent term $f_l\exp(-W_l)$.

Following the above ensemble averaging procedure for $\hat{K}$ and $\hat{\mu}$ the atomic-motion effect can be included in the equations of DFB x-ray laser, Eqs. (12) and (13), by replacing K_n and μ_n by $K_n \exp(-W_n)$ and $\mu_n \exp(-W_n)$, respectively,

$$\frac{\partial}{\partial z}\varepsilon_+ + \frac{1}{c}\frac{\partial}{\partial t}\varepsilon_+ - (g_+ - i\delta - \mu_0 - iK_0)\varepsilon_+ + e^{-W_n}(\mu_n + iK_n)\varepsilon_- = 0 , \quad (22)$$

$$-\frac{\partial}{\partial z}\varepsilon_- + \frac{1}{c}\frac{\partial}{\partial t}\varepsilon_- - (g_- - i\delta - \mu_0 - iK_0)\varepsilon_- + e^{-W_n}(\mu_n^* + iK_n^*)\varepsilon_+ = 0 , \quad (23)$$

where we use that $W_0 = 0$.

The inclusion of the atomic motion by a Debye-Waller factor was verified experimentally in anomalous transmission of x-rays by multiple diffraction (the Borrmann effect).[10,13] From Eq. (20) we find that even at zero temperature, where $n_{qs} = 0$, $W_i \neq 0$ and the zero-point motion influences Eqs. (22) and (23). In the Sec. IV, Eqs. (22) and (23) will be used to analyze the threshold conditions of DFB x-ray laser.

IV. THRESHOLD AND SELECTIVITY CONDITIONS

We now find the effect of absorption and atomic motion on the threshold gain and selected resonance frequency. The system at threshold is presented by the solution of Eqs. (22) and (23) at steady state,[6]

$$\frac{d}{dz}\varepsilon_+ - (g_- - i\delta - \mu_0 - iK_0)\varepsilon_- + e^{-W_n}(\mu_n + iK_n)\varepsilon_- = 0 , \quad (24)$$

$$-\frac{d}{dz}\varepsilon_- - (g_- - i\delta - \mu_0 - iK_0)\varepsilon_- + e^{-W_n}(\mu_n^* + iK_n^*)\varepsilon_+ = 0 , \quad (25)$$

where g is identified as a threshold gain and δ as the selected frequency.

The coupled waves Eqs. (24) and (25) describe the spatial variation of transmitted- and reflected-wave amplitudes in a beam-channeling DFB medium. For a slab of length L centered at $z = 0$, the accompanying boundary conditions read: $\varepsilon_+(-L/2) = \varepsilon_-(L/2) = 0$ and no external radiation sources are assumed. The corresponding eigenvalue solutions to Eqs. (24) and (25) for the case that K_n and μ_n are real numbers are found directly,

$$\varepsilon_+(z) = e^{gz/2}\sinh[\lambda(z + L/2)] , \quad (26)$$

$$\varepsilon_-(z) = \pm e^{gz/2}\sinh[\lambda(z - L/2)] , \quad (27)$$

where

$$\lambda = \left\{ \left| \frac{g}{2} - i\delta - iK_0 - \mu_0 \right|^2 + e^{-2W_n}(K_n - i\mu_n)^2 \right\}^{1/2} \quad (28)$$

and the dispersion relation is

$$\left| \lambda - \frac{g}{2} + i\delta + iK_0 + \mu_0 \right| + \left| \lambda - \frac{g}{2} - i\delta - iK_0 - \mu_0 \right| \times e^{-2\lambda L} = 0 . \quad (29)$$

A formal solution of allowed resonance frequencies δ and threshold values g can be obtained by inserting Eqs. (26) and (27) in Eq. (24),

$$\lambda = \pm(iK_n + \mu_n)e^{-W_n}\sinh(\lambda L) , \quad (30)$$

$$\frac{g}{2} - i\delta = (iK_0 + \mu_0) \pm (iK_n + \mu_n)e^{-W_n}\cosh(\lambda L) . \quad (31)$$

Equation (30) determines λ. Substitution of λ into Eq. (31) and equating real and imaginary parts yields the allowed δ and g.

Approximate formulas can be obtained in the limit of strong reflections: $(K_n L)^2 \gg (gL)^2 + 1$ and $|\lambda L| \ll 1$. Upon expanding Eq. (30) in this limit and using the expression for λ we find for the first resonance that

$$\delta = -K_0 + [\mu_0^2 + e^{-2W_n}(K_n^2 - \mu_n^2)]^{1/2} , \quad (32)$$

and the threshold gain condition g_t is

$$g_t = 2\mu_0 + \frac{\left| \frac{6K_n e^{W_n}}{(K_n^2 + \mu_n^2)L^3} - 2e^{-2W_n}K_n\mu_n \right|}{[\mu_0^2 + e^{-2W_n}(K_n^2 - \mu_n^2)]^{1/2}} . \quad (33)$$

Equations (32) and (33) can be simplified for the typical case of stronger reflection compared to absorption: $K_n^2 \gg \mu_0^2, \mu_n^2$. For this case,

$$\delta = -K_0 + K_n e^{-W_n} , \quad (34)$$

$$g_t = \frac{6e^{2W_n}}{K_n^2 L^3} + 2(\mu_0 - e^{-W_n}\mu_n) . \quad (35)$$

The threshold gain in Eq. (35) includes two independent terms; the first term is due to reflection,[6] the second one is due to absorption. In a one-passage amplification system (with no reflections) the absorption is with the average absorption coefficient μ_0 which is large for x rays, $\mu_0 > 10\ \text{cm}^{-1}$.[11] In the Bragg-reflection coupling system, standing waves are generated with nodes on the atomic sites and the absorption, located mainly near the atomic sites, is strongly reduced. For this case at low temperature compare to the Debye temperature, where $\exp(-W_n) \sim 1$, μ_n is of the order of μ_0 and g_t due to absorption is strongly reduced compared to μ_0. As the temperature increases the atomic displacement and the absorption increases, the reflectivity of the atomic planes K_n is reduced to $K_n \exp(-W_n)$; thus the threshold-gain condition is increased. Section V is devoted to numerical results and discussion of the threshold-gain condition in Eq. (35).

V. DISCUSSION

We first consider the threshold-gain condition by neglecting the atomic motion $\exp(-W_n)=1$. From Eq. (35) we can write $g_t=6/(K_n^2L^3)+2(\mu_0-\mu_n)$. As a numerical example let us consider a periodic absorption function $\mu(z)=\mu(z+a)$ defined by

$$\mu(z)=\begin{cases}(a/b)\mu_0, & z \le b/2 \\ 0, & b/2<|z|<(a-b)/2\end{cases}, \tag{36}$$

where b is the region of absorption around an atomic site located at $z=0$ and $b \ll a$. We use the Fourier expansion Eq. (8) to obtain

$$\mu_n=\mu_0\frac{\sin(n\pi b/a)}{n\pi b/a} . \tag{37}$$

From Eq. (37) as $b/a \to 0$, $\mu_n \to \mu_0$ for all n and the absorption $\mu_0-\mu_n$ is drastically reduced. Standing waves are generated with nodes on the atomic sites reducing the absorption located on the atomic sites and the threshold gain. As the order of Bragg reflection n increases, μ_n decreases relative to μ_0 and g_t due to absorption is increased. Thus the lowest threshold is obtained for the first-order Bragg reflections, $n=1$. From numerical calculation of the anomalous absorption in a germanium single crystal the value of $1-\mu_n/\mu_0$ can be of the order of 10^{-3}.[14] Thus, using Eq. (37) for $n=1$, $a=3$ Å gives $b=0.1$ Å and the absorption is mainly due to the tightly bound electrons located very close to the atomic sites.

The threshold-gain condition due to reflection can be evaluated using the reflection function $K(z)$ with a modulated atomic electron density: $n_e(z)=n_0[1+\cos(2k_Bz)]$.[6] Applying the Fourier expansion, Eq. (8), for $K(z)$ we obtain $K_0=2\pi e^2n_0/cm\omega_B$ and $K_1=+K_0/2$. Typically K_0 is on the order of 10^4 cm^{-1} in a number of crystalline samples used in channeling studies, for example, silicon and diamond, where n_0 is approximately the crystal bound-electron density. For first-order Bragg reflections $n=1$ and $L=0.1$ cm the value of g_t due to reflection is 2×10^{-4} cm^{-1}.[6] In crystals with low atomic numbers, e.g., LiH, $\mu_0 \sim 10$ cm^{-1} and for $1-\mu_1/\mu_0 \sim 10^{-3}$ the value of g_t due to absorption is 10^{-2} cm^{-1}. Thus, the main contribution here to the threshold-gain condition is absorption. But as L decreases below 200 μm the reflection contribution to g_t exceeds the absorption one.

It is shown in Refs. 15 and 16 that by applying a diffraction scheme from several sets of atomic planes which satisfy the Bragg condition simultaneously, it is possible to reduce the absorption of the radiation. In this method, called the multibeam Borrmann effect, standing waves are generated in several directions relative to the atomic site, generating larger nodal regions in radiation fields and the absorption for some of the radiation modes can be reduced by a factor of 10^{-4}.[16] For this case and $\mu_0 \sim 10$ cm^{-1}, g_t due to absorption can be reduced to 10^{-3} cm^{-1}.

The inclusion of the atomic motion in Eq. (35) is through the Debye-Waller factor and is related to the average displacement U, where $U^2=\langle(U_j^{(z)})^2\rangle$ decreases with the increase in the Debye temperature T_D. For a crystal with a high Debye temperature W_n due to the zero-point motion can be as slow as $W_n \sim 10^{-3}n^2$.[14] Thus, for $n=1$ and temperatures $T \ll T_D$ the zero-point motion does not change g_t appreciatively. But as the temperature increases above the Debye temperature the phonon occupation numbers in Eq. (20) introduce in W_1 a temperature dependence proportional to $1+2T/T_D$. This thermal motion has a strong effect on g_t due to absorption which takes the form of $2\mu_0[1-\exp(-W_n)]$ for $\mu_0 \sim \mu_n$, and for large W_n the absorption is $2\mu_0$. The thermal motion reduces the reflectivity of the atomic planes to $K_n\exp(-W_n)$ and the total g_t is increased. Thus, in the DFB scheme of x-ray laser one should consider temperatures $T \ll T_D$ with $n=1$. Furthermore, by applying the multibeam Borrmann effect together with the DFB scheme the atomic-motion effect and the threshold-gain condition can be further reduced.

For the case the gain g is larger than the threshold gain g_t the radiation fields $\varepsilon_\pm$ increase with time as $\exp[(g-g_t)ct/2]$ in the linear range. Thus, an amplification factor $(g-g_t)ct/2 \sim 1$ is obtained for a beam-pulse duration of 50 ns, $L=0.1$ cm, and $\mu_0 \sim 10$ cm^{-1} for $g \sim 10^{-2}$ cm^{-1} in the DFB scheme and by including multibeam Borrmann effect for $g \sim 2\times10^{-3}$ cm^{-1}. These results should be compared to the gain $(g-\mu_0)L \sim 1$ obtained in a one passage amplification, wherefore $L=0.1$ cm and $\mu_0 \sim 10$ cm^{-1}, $g \sim 20$ cm^{-1}. Thus, in spite of the limitations on g_t due to the absorption, in terms of beam-current requirements the DFB mechanism in beam channeling has possible application in reducing current requirements by many orders of magnitude.

In the present paper we pointed out that the combined effects of DFB mechanism and multibeam Borrmann anomalous transmission can be useful in reducing radiation absorption. Threshold conditions for these combined effects for specific geometry of reflection planes require further study.

ACKNOWLEDGMENTS

This work was supported by the Naval Research Laboratory (NRL) and the Strategic Defense Initiative Organization (SDIO).

---

*On leave from the Nuclear Research Center, Negev, P.O. Box 9001, Beer Sheva, Israel.

[1] J. U. Andersen, E. Bonderup, and R. H. Pantell, Annu. Rev. Nucl. Part. Sci. 33, 453 (1983); V. V. Beloshitsky and F. F. Komarov, Phys. Rep. 93, 117 (1982); G. Kurizki and J. K. McIver, Phys. Rev. B 32, 4358 (1985).

[2] R. K. Klein *et al.*, Phys. Rev. B 31, 68 (1985); B. L. Berman, B. A. Dahling, S. Datz, J. O. Kephart, R. K. Klein, R. H. Pan-

tell, and H. Park, Nucl. Instrum. Methods B **10/11**, 611 (1985).
[3]V. V. Beloshitsky and M. A. Kumakhov, Phys. Lett. A **69**, 247 (1978).
[4]G. Kurizki, M. Strauss, J. Oreg, and N. Rostoker, Phys. Rev. A **35**, 3424 (1987).
[5]Y. H. Ohtsuki, Nucl. Instrum. Methods B **2**, 80 (1984).
[6]M. Strauss, P. Amendt, N. Rostoker, and A. Ron, Appl. Phys. Lett. **52**, 866 (1988).
[7]H. Kogelnik and C. V. Shank, Appl. Phys. Lett. **18**, 152 (1971); J. Appl. Phys. **43**, 2327 (1972).
[8]A. Yariv, Appl. Phys. Lett. **25**, 105 (1974).
[9]V. G. Borrmann and W. Hartwig, Z. Kristallogr., Kristallgeom. Kristallphys. Kristallchem. **121**, 401 (1965).
[10]B. W. Batterman, Rev. Mod. Phys. **36**, 681 (1964).
[11]L. V. Azaroff, *Elements of X-Ray Crystallography* (McGraw-Hill, New York, 1968).
[12]J. P. Hannon and G. T. Tramell, Opt. Commun. **15**, 330 (1975).
[13]B. W. Batterman, Phys. Rev. **126**, 1461 (1962); B. W. Batterman and D. R. Chipman, *ibid.* **127**, 690 (1962); J. Appl. Phys. **34**, 2716 (1963).
[14]H. Wagenfeld, J. Appl. Phys. **33**, 2907 (1962).
[15]T. Joko and A. Fukuhara, J. Phys. Soc. Jpn. **22**, 597 (1967); E. J. Seccocio and A. Zajac, Phys. Rev. **139**, 225 (1965); J. T. Hutton, J. P. Hannon, and G. T. Trammell, Phys. Rev. A **37**, 4280 (1988).
[16]T. C. Huang, M. H. Tillinger, and B. Post, Z. Naturforsch **28A**, 600 (1973).
[17]M. Strauss, P. Amendt, H. U. Rahman, and N. Rostoker, Phys. Rev. Lett. **55**, 406 (1985); M. Strauss, Phys. Rev. A **38**, 1358 (1988).
[18]N. W. Ashcroft and N. D. Mermin, *Solid State Physics* (Holt, Rinehart and Winston, New York, 1976), pp. 780-795.

Radiation guiding in channeling beam x-ray laser by Bragg reflection coupling

M. Strauss* and N. Rostoker
Department of Physics, University of California, Irvine, California 92717
(Received 5 June 1989)

The effects of radiation guiding on an electron-beam channeling x-ray laser are investigated. An essential feature of this laser is distributed feedback induced by Bragg reflections. Using the Maxwell-Bloch scheme including the transverse Laplacian it is shown that reflection guiding and absorption guiding can avoid the diffraction of the amplified radiation out of the amplification medium for a beam radius in the range of 100–1000 Å. This opens the possibility of considering a channeling x-ray laser with high current density (10^5 A/cm^2), low emittance, but with very small total current (10 μA), similar to the beam used in scanning electron microscopy. On the other hand, gain guiding can avoid radiation diffraction in such small beam systems, but only with a further increase in the requirements on the beam current density. It is noted that planar superlattice crystals with a periodic structure of the order of 100 Å transverse to the beam propagation can be useful for radiation guiding.

I. INTRODUCTION

A relativistic electron beam propagating through planar or axial channels in a crystal free of imperfections may populate bound transverse energy eigenstates.[1] Spontaneous dipolar transitions between these discrete eigenstates have been shown experimentally to yield narrow-width, highly polarized, and intense x-ray radiation which is strongly forward peaked.[2] Previous estimates suggest that for using the channeling mechanism as a *coherent x-ray source in a one-pass amplification* scheme even modest gains may require very high current density in the range of 10^7–10^8 A/cm^2.[3–5]

An efficient scheme to significantly reduce the gain requirements for a channeling x-ray laser was proposed based on the concept of a distributed feedback laser (DFB), which is supplied by multiple Bragg reflections of the radiation.[6] The advantages of using DFB lasers includes the high degree of spectral selectivity with low gain per pass without the need for cavity mirrors. The radiation tunability is obtained by adjusting the electron-beam energy so that the Doppler up-shifted radiation can be tuned onto a line in the DFB model spectrum near the Bragg reflection frequency. These mirrorlike structures have the possibility to reduce high-beam-current-density requirements to the range 10^4–10^5 A/cm^2. High-current-density beams (10^5–10^6 A/cm^2, dc) with very low emittance have been developed for scanning electron microscopy.[7] In such systems the electron-beam source is a field emission type with very small beam radius (10 Å) and thus with very low total current. The total current is limited by the requirement that the beam, which is dc, should not damage the cathode. The beam emittance is about 10^{-7} rad cm, which is about 3 orders of magnitude lower than that for the best conventional electron sources. The beam expands after emission, but is routinely refocused to 10^6 A/cm^2 with a magnetic lens. For present purposes, the beam may be pulsed, in which case it should be possible to increase the current without damaging the cathode. Presumably this can be done without increasing the emittance; however, this remains to be documented in the laboratory. We assume that with a pulsed emitter the current can be increased by a factor of 10^3 (from 30 nA dc to 30 μA in a 10-nsec pulse) so that a current density of 10^5 A/cm^2 can be produced over a 1000-Å beam radius. For such a small beam radius one must consider a mechanism to avoid radiation diffraction out of the amplification medium. For a system of length L, the Fesnel spatial guiding condition is $F_0=\pi a^2/\lambda L \gg 1$, where λ is the radiation wavelength and a is the beam radius. For a system with $L=0.1$ cm, $a=1000$ Å, and $\lambda=3$ Å, then $F_0<1$ and radiation guiding cannot be maintained. In this paper we identify an efficient scheme for radiation guiding for such small radius beams.

We consider the channeling DFB scheme using the Maxwell-Bloch equations including the effects of radiation reflection, absorption, and diffraction. In Ref. 6 only a one-dimensional effect along the amplification direction is considered. In this paper we extend the results to a three-dimensional treatment including diffraction effects as guiding, and a multimode expansion introduced due to the small radius of the beam. Radiation diffraction is presented by including the transverse Laplacian and finding the eigenmode solutions at threshold gain condition. The channeling lasant medium is assumed to be surrounded by a nonlasant medium for a transverse square beam profile. The surrounding medium can be the same channeling crystal where Bragg reflections are avoided by impurities or dislocations, or a medium with a higher atomic number. It is found that for a beam radius in the range 100–1000 Å, reflection guiding and absorption guiding[8] can maintain the amplification of modes guided in the lasant medium. This avoids the diffraction of the radiation out of the amplification volume independent of the system length or gain factor. We also look for a gain guiding mechanism. We find that small radius gain guiding further increases the requirements on the

beam current density.

It is noted that radiation guiding by reflections or absorptions can be maintained by a planar superlattice structure transverse to the electron-beam propagation, where lasant regions of 100–1000 Å wide are surrounded by nonlasant guiding regions. The radiation guiding in the other transverse dimension can be Fresnel guiding ($F_0 \gg 1$) in a range of 1 μm. Thus radiation guiding in a beam of dimension 100 Å $\times$ 1 μm can be maintained with a total beam current of 10 μA and a current density of 10^5 A/cm^2.

Some of the system parameters considered here are optimistic and a theoretical and an experimental effort should be performed to identify the physical mechanisms that can improve their values. The occupation length of the bound states is taken in the range 100–1000 μm. At room temperature this value is of the order of 50 μm and limits the cavity length. Cooling the crystal or increasing the beam particle energy may increase, to some extent, its value. It is also possible to increase the occupational length by applying a set of successive foils in the longitudinal direction to recapture the bound-state population. It is assumed that the population inversion in the lasing states is of the order of unity. An exact treatment of the population of the bound states may reduce this value and increase the current density requirements. Another optimistic parameter is the coherence length c/Γ, where $1/\Gamma$ is the decay time of the state polarization, and it is taken to be of the order of the occupation length. In general, the coherence length is smaller or equal to the occupation length and an effort should be made to increase their values. In this paper, we indicate the mechanisms which can be of interest for channeling x-ray lasers in high beam current densities and do not represent a complete solution of the problem.

The plan of the paper is as follows. In Sec. II we consider the DFB equations of motion for the lasant channeling medium. Eigenmodes solutions and the guiding conditions for the DFB system, including the nonlasant medium, are derived in Sec. III. The guiding in a one-pass system is considered in Sec. IV. Summary and conclusions are given in Sec. V.

II. DIFFRACTION MODEL IN A DFB X-RAY LASER

In this section we consider the radiation propagation in the lasant channeling medium. The inclusion of the surrounding nonlasant medium is presented in the following sections. We begin by characterizing the set of channeling transverse eigenstates as a two-level system with states $|1\rangle$ and $|2\rangle$, W and $\hbar\omega_0 = \epsilon_2 - \epsilon_1$ are the population and energy differences, respectively.[4] The directions of beam channeling and Bragg reflections are taken in the z direction. The Doppler up-shifted radiation frequency $\omega = \omega_0 [1 - v/c] \simeq 2\gamma^2 \omega_0$ in the forward direction is chosen to closely match the nth-order Bragg frequency $\omega = n\omega_B$, where v is the channeling electron speed, $\omega_B = \pi c/b$, and b is the periodic reflection plane spacing. Consequently, the channeling radiation can be tuned to satisfy the Bragg reflection condition and induce distributed feedback in the channeling crystal.[5]

The electric E and polarization P fields are taken in transverse x direction and are defined in terms of forward and backward traveling waves

$$E = \epsilon_+ e^{-i(\omega t - z/c)} + \epsilon_- e^{-i(\omega t + z/c)} + \text{c.c.} ,$$
$$P = p_+ e^{-i(\omega t - z/c)} + p_- e^{-i(\omega t + z/c)} + \text{c.c.} , \tag{1}$$

where ω is the electromagnetic wave frequency, $\epsilon_\pm$ and $p_\pm$ are slowly varying complex amplitudes depending on $\rho = (x,y)$, z, and t.

The radiation propagation is considered in the framework of the Maxwell-Bloch set of equations. The Maxwell wave equation is

$$\nabla^2 \mathbf{E} - \frac{1}{c^2}\frac{\partial^2}{\partial t^2}\mathbf{E} = \frac{4\pi}{c^2}\frac{\partial}{\partial t}\left[\frac{\partial}{\partial t}\mathbf{P} + c\nabla\times\mathbf{M} + \mathbf{J}\right] , \tag{2}$$

where the magnetization $\mathbf{M} = \mathbf{P}\times\mathbf{v}/c$.[4] The crystal-induced current $\mathbf{J}$ can be represented as[6,9]

$$\frac{\partial}{\partial t}\mathbf{J} = \frac{c}{2\pi}\left[\omega K \mathbf{E} + \mu\frac{\partial \mathbf{E}}{\partial t}\right] , \tag{3}$$

where $K = 2\pi e^2 n_c / c m_e \omega$ is the reflection function with n_c the spatially modulated atomic electron density, and μ is the modulated absorption function. An average is carried out on K and μ over the transverse dependence $\rho = (x,y)$ so that $K(z) = K(z+a)$ and $\mu(z) = \mu(z+a)$ are periodic functions in the z direction. Inserting Eq. (3) in Eq. (2) and using Eq. (1) we obtain

$$\sum_{\eta=\pm 1} e^{i\eta kz}\left[\left[-\frac{i}{2k}\nabla_\perp^2 + \eta\frac{\partial}{\partial z} - \frac{1}{c}\frac{\partial}{\partial t} + \mu + iK\right]\epsilon_\eta - 2\pi i\frac{\omega}{c}(1 - \eta v/c)P_\eta\right] = 0 , \tag{4}$$

where ϵ_η and P_η for $\eta = \pm 1$ are $\epsilon_\pm$ and $P_\pm$, respectively. Here $k = \omega/c$ and the second-order derivatives with respect to z and t are ignored because $\partial^2\epsilon/\partial t^2 \ll \omega\partial\epsilon/\partial t$ and $\partial^2\epsilon/\partial z^2 \ll k\partial\epsilon/\partial z$. The diffraction effect in Eq. (4) is represented by the transverse Laplacian $\nabla_\perp^2$.

Equation (4) is supplemented by the Bloch equation for P_-,[10]

$$\frac{\partial}{\partial t}P_- + v\frac{\partial}{\partial z}P_- = i\Delta_- P_- - i(1 \mp v/c)d^2 n_b W(\epsilon_-/\hbar) - \Gamma P_- , \tag{5}$$

where $d = e\langle 1|x|2\rangle$ is the electric dipole moment, n_b is the beam number density depending on the transverse coordinate ρ, Γ is a phenomenological damping constant related to the channeling coherence length c/Γ, $\Delta_- = \omega(1 \mp v/c) - \omega_0$ is a detuning frequency, and v/c represents a magnetic dipole interaction correction. In the limit of short coherence length V/Γ the left-hand side of Eq. (5) is small and near resonance ($\Delta_- = 0$ and $\omega \simeq 2\gamma^2\omega_0$):

$$P_- = -id^2 n_b W(1 - v/c)\epsilon_-/\hbar\Gamma . \tag{6}$$

In this limit $\Delta_- \sim \omega$, $\Delta_- \gg \Gamma$, and in the case of low gain P_- can be ignored in Eq. (4). Substituting Eq. (6) in Eq. (4) we obtain

$$\sum_{\eta=\pm 1} e^{i\eta kz}\left[-\frac{i}{2k}\nabla_\perp^2+\eta\frac{\partial}{\partial z}+\frac{1}{c}\frac{\partial}{\partial t}+\mu+iK-g_\eta\right]\epsilon_\eta=0\ , \tag{7}$$

where g_η for $\eta=+1$ is $g_+=g=2\pi\omega d_1^2 n_b W/\hbar c\Gamma$ and is the forward gain factor with $d_1=d(1-v/c)$, and g_η for $\eta=-1$ is $g_-=0$ and is the backward gain factor.[6,11] The gain g_+ includes the beam transverse profile and depends on $\rho=(x,y)$.

In the following we obtain the equation of motion for a DFB x-ray laser by using the resonance parts of Eq. (7). Notice that K and μ are periodic functions in z and for $f(z)=f(z+a)$ we can use the Fourier series expansion

$$f(z)=\sum_{l=-\infty}^{\infty} f_l e^{2ilk_B z}\ , \tag{8}$$

where $k_B=\omega_B/c=\pi/b$ and

$$f_l=\frac{1}{b}\int_{-b/2}^{b/2} dz\, f(z)e^{-2ilk_B z}\ . \tag{9}$$

We insert the Fourier expansion Eq. (8) for $K(z)$ and $\mu(z)$ in Eq. (7). For the case that the radiation frequency is close to the lth-order Bragg reflection condition $k\sim lk_B$, and ignoring highly oscillatory terms, we obtain from Eq. (7)

$$-\frac{i}{2k}\nabla_\perp^2\epsilon_+ +\frac{\partial}{\partial z}\epsilon_+ +\frac{1}{c}\frac{\partial\epsilon_+}{\partial t} -(g_+ -i\delta-\nu_0)\epsilon_+ +\nu_-\epsilon_-=0\ , \tag{10}$$

$$-\frac{i}{2k}\nabla_\perp^2\epsilon_- -\frac{\partial}{\partial z}\epsilon_- +\frac{1}{c}\frac{\partial\epsilon_-}{\partial t} -(g_- -i\delta-\nu_0)\epsilon_- +\nu_+\epsilon_+=0\ , \tag{11}$$

where Eq. (10) and Eq. (11) are obtained from Eq. (7) for $\eta=+1$ and $\eta=-1$, respectively. In Eqs. (10) and (11) we redefined $\epsilon_\pm$ as $\epsilon_\pm\exp[\mp i(k-lk_B)z]$, and $\delta=lk_B-k$ is the small detuning from the lth-order Bragg reflection.[6] Here $\nu_0=\mu_0+iK_0$, $\nu_-=\mu_l+iK_l$, and $\nu_+=\mu_l^*+iK_l^*$, where we used the fact that K and μ are real functions, i.e., $K_{-l}=K_l^*$ and $\mu_{-l}=\mu_l^*$.

To include the atomic displacement effects and thermal motion $K_l\to K_l\exp(-W_l)$ and $\mu_l\to\mu_l\exp(-W_l)$, where W_l is the Debye-Waller factor of order l.[9,12] Here $W_l=2(lk_B)^2\langle(U^z)^2\rangle$ and $\langle(U^z)^2\rangle$ is the ensemble average of the square of the atomic displacement in the z direction.[13]

The coupled set Eqs. (10) and (11) are the DFB equations of motion, where diffraction effects are presented by the transverse Laplacian and by the transverse beam profile in $g_\pm$. In the following section eigenmode solutions of Eqs. (10) and (11) at threshold are considered and the conditions for radiation guiding are derived.

III. EIGENMODES AND RADIATION GUIDING IN DFB SYSTEMS

The system at threshold is presented by the set of equations (10) and (11) at steady state,[6,11]

$$-\frac{i}{2k}\nabla_\perp^2\epsilon_\pm\pm\frac{\partial}{\partial z}\epsilon_\pm-(g_\pm-i\delta-\nu_0)\epsilon_\pm+\nu\epsilon_\mp=0\ , \tag{12}$$

where for the lasant channeling medium $\nu_0=\mu_0+iK_0$, $\nu=\mu_l+iK_l$, and for simplicity we take K_l and μ_l to be real.

To extend Eq. (12) for the surrounding nonlasant medium we define for that region $\nu_0=\tilde{\nu}_0=\tilde{\mu}_0+i\tilde{K}_0$, where $\tilde{\mu}_0$ and $\tilde{K}_0$ are the average absorption and reflection coefficient of the nonlasant medium, respectively. We further ignore the gain ($g_\pm=0$) and Bragg reflections ($\nu=0$) in the nonlasant medium. Equation (12) is a coupled set of Schrödinger-type equations with a complex potential.

A. Eigenmode solutions

For a transverse beam profile in the lasant medium of the form $\frac{1}{2}[f_+(x)+h_+(y)]$ the gain factors are

$$g_\pm(x,y)=\frac{g}{2}[f_\pm(x)+h_\pm(y)]\ , \tag{13}$$

where $g_-(x,y)=0$ or $f_-(x)=h_-(y)=0$. The eigenmode solution (n,m) for Eq. (12) can be written as

$$\epsilon_\pm^{(n,m)}(\rho,z)=e^{q_{n,m}z}U_\pm^{(n)}(x)V_\pm^{(m)}(y)\ , \tag{14}$$

where $q_{n,m}=\frac{1}{2}(q_n+q_m)$ and the eigenstates equations of motion are

$$\left[-\frac{i}{k}\frac{d^2}{dx^2}\pm q_n-[g\cdot f_\pm(x)-i\delta-\nu_0]\right]U_\pm^{(n)}(x)+\nu U_\mp^{(n)}(x)=0\ , \tag{15}$$

$$\left[-\frac{i}{k}\frac{d^2}{dy^2}\pm q_m-[g\cdot h_\pm(y)-i\delta-\nu_0]\right]V_\pm^{(m)}(y)+\nu V_\mp^{(m)}(y)=0\ . \tag{16}$$

For explicit solutions we consider in the following the case of a transverse square well gain profile: $f_+(x)=h_+(y)=1$ for the lasant medium $|x|<a$ and $|y|<a$, and zero gain outside this well. For this case the eigenstate solutions in the x and y direction are similar, i.e., $V_\pm^{(n)}(y)=U_\pm^{(n)}(y)$. For the x direction the symmetric solutions of Eq. (15) are

$$U_\pm^{(n)}(x)=\begin{cases} A_\pm(e^{i\alpha_n x}+e^{-i\alpha_n x}), & |x|\le a \\ B_\pm e^{i\beta_n x}, & x\ge a \end{cases} \tag{17}$$

where $\mathrm{Im}(\beta_n)>0$ in order that $\exp(i\beta_n x)\to 0$ for $x\to\infty$. Antisymmetric solutions of Eq. (15) can be obtained in a similar way to the symmetric solutions, but are not considered in the following.

To obtain a closed set of equations for α_n, β_n, and q_n

we insert Eq. (17) for the lasant region ($x < a$) in Eq. (15):

$$\left| \frac{i\alpha_n^2}{k} \mp q_n - g_\pm + i\delta + \nu_0 \right| A_- + \nu A_\pm = 0 , \tag{18}$$

where $g_+ = g$ and $g_- = 0$ for $x < a$. From the condition on the determinant of the coefficients A_- in Eq. (18) to be zero we obtain

$$\left| q_n - g_- + i\delta + \nu_0 + \frac{i\alpha_n^2}{k} \right| \times \left| -q_n - g_- + i\delta + \nu_0 + \frac{i\alpha_n^2}{k} \right| - \nu^2 = 0 . \tag{19}$$

In a similar way we can get for the nonlasant region $x > a$, where $g_\pm = 0$ and $\nu = 0$ the condition

$$\left| q_n + i\delta + \tilde{\nu}_0 + \frac{i\beta_n^2}{k} \right| \left| -q_n + i\delta + \tilde{\nu}_0 + \frac{i\beta_n^2}{k} \right| = 0 . \tag{20}$$

The dispersion relation is obtained from the continuity conditions on $U_\pm(x)$ and $dU_\pm(x)/dx$ at $x = a$

$$\tan(\alpha_n a) = -\frac{i\beta_n}{\alpha_n} . \tag{21}$$

The closed set of equations (19)–(21) can be solved for α_n, β_n, and q_n.

Assuming that α_n is known then from Eq. (19), we can solve for q_n in terms of α_n

$$q_n^{(1)} = \frac{g}{2} + \lambda_n , \quad q_n^{(2)} = \frac{g}{2} - \lambda_n , \tag{22}$$

where

$$\lambda_n = \left[\left| \frac{g}{2} - i\delta - \nu_0 - \frac{i\alpha_n^2}{k} \right|^2 - \nu^2 \right]^{1/2} . \tag{23}$$

For a slab of length L centered at $z = 0$, the accompanying boundary conditions read $\epsilon_\pm(z = \mp L/2) = 0$ and no external radiation sources are assumed. The eigenmode solutions in the range $x < a$ and $y < a$ consistent with the boundary condition are[6,11]

$$\begin{aligned} \epsilon_+^{(n,m)}(\rho, z) &= e^{gz/2} \sinh[\lambda_{n,m}(z - L/2)] \\ &\quad \times \cos(\alpha_n x) \cos(\alpha_m y) , \\ \epsilon_-^{(n,m)}(\rho, z) &= \mp e^{gz/2} \sinh[\lambda_{n,m}(z - L/2)] \\ &\quad \times \cos(\alpha_n x) \cos(\alpha_m y) , \end{aligned} \tag{24}$$

where $\lambda_{n,m} = (\lambda_n + \lambda_m)/2$. A formal solution for the allowed resonance frequencies δ and threshold values g for the eigenstate (n,m) can be obtained by inserting Eq. (24) in the equation for $\epsilon_\pm$ in Eq. (12), and we obtain that

$$\lambda_{n,m} = \mp \nu \sinh(\lambda_{n,m} L) , \tag{25}$$

$$\frac{g}{2} - i\delta = \nu_0 + \frac{1}{2k}(\alpha_n^2 + \alpha_m^2) \mp \nu \cosh(\lambda_{n,m} L) . \tag{26}$$

The coupled equations (25) and (26) yield the allowed δ and g for the mode (n,m).

Approximate solutions of Eqs. (25) and (26) can be obtained in the limit of strong reflections ($|K_l L|^2 \gg 1 + (gL)^2$ and $|\lambda_{n,m} L| \ll 1$. Upon expanding Eq. (25) in this limit for $n = m$ and using that $\mu_0^2, \mu_l^2 \ll K_l^2$, we obtain the lowest threshold values for δ and g for the states (n,n)

$$\delta_t^{(n,n)} = -K_0 + K_l - \frac{1}{k}\mathrm{Re}(\alpha_n^2) , \tag{27}$$

$$g_t^{(n,n)} = \frac{6}{K_l^2 L^3} + 2(\mu_0 - \mu_l) - \frac{2}{k}\mathrm{Im}(\alpha_n^2) . \tag{28}$$

The first term in the threshold gain Eq.(28) is due to reflections. The second term in Eq. (28) is due to reduced absorption of the standing radiation waves generated with nodes on the atomic sites and is similar to the Borrmann anomalous transmission effect.[9] From numerical calculation of the anomalous absorption in single crystal the value of $1 - \mu_l/\mu_0$ can be of the order of 10^{-3}.[12] Thus, for $\mu_0 \sim 10\ \mathrm{cm}^{-1}$, the threshold gain due to absorption can be reduced to the order of $10^{-2}\ \mathrm{cm}^{-1}$. The real and imaginary parts of α_n^2 in Eqs. (27) and (28) are the mode contributions to the selectivity and threshold gain, respectively. In the following, limiting values of α_n are considered and the conditions for radiation guiding in DFB x-ray lasers are derived.

B. Guiding conditions

For the square well gain profile guiding solutions are obtained for $|\alpha_n/\beta_n| \ll 1$. For this case we obtain from the dispersion relation Eq. (21) that $\alpha_n a = (n + \frac{1}{2})\pi$ and the threshold values in the strong reflection limit Eqs. (27) and (28) are

$$\delta_t^{(n,n)} = -K_0 + K_l - \frac{\pi^2}{ka^2}(n + \tfrac{1}{2})^2 , \tag{29}$$

$$g_t^{(n,n)} = \frac{6}{K_l^2 L^3} + 2(\mu_0 - \mu_l) . \tag{30}$$

The threshold gain in Eq. (30) is independent of n. But for a transverse gain profile which is maximized at the center $x = y = 0$, then the threshold gain would increase with n.

The condition for radiation guiding is that $|e^{i(\beta_n a)}| \ll 1$ or $\mathrm{Im}(\beta_n a) \gg 1$. For low values of n, $\alpha_n a \sim 1$ and the condition for guiding is consistent with the condition $|\alpha_n/\beta_n| \ll 1$. To calculate β_n we use Eq. (20) in the strong reflection limit [$(K_l L)^2 \gg 1 + (g/2)^2$, $|\lambda_n L| \ll 1$], where q_n, Eq. (22), can be ignored. The equation for β_n^2 is

$$i\delta + \tilde{\mu}_0 - i\tilde{K}_0 + \frac{i\beta_n^2}{k} = 0 . \tag{31}$$

From Eq. (29) $\delta \approx -K_0 + K_l$ and the solution for β in Eq. (31) is

$$\beta_n = [ik\tilde{\mu}_0 - k(\tilde{K}_0 - K_0 + K_l)]^{1/2} . \tag{32}$$

From Eq. (32) there are two mechanisms for radiation guiding independent of the gain or length of the system: the absorption guiding and the reflection guiding.[3] The

absorption guiding condition is obtained for $\tilde{\mu}_0 > |\tilde{K}_0 - K_0 + K_l|$ and $\mathrm{Im}(\beta_n a) \simeq (ka^2\tilde{\mu}_0/2)^{1/2} \gg 1$, where $\tilde{\mu}_0$ is the average absorption coefficient of the nonlasant medium. For this case the effective Fresnel number $F_\mu = \pi a^2 \tilde{\mu}_0/\lambda > 1$, with an effective length $L_{\mathrm{eff}} = 1/\tilde{\mu}_0$. The reflection guiding is obtained for $\tilde{K}_0 > K_0 - K_l \tilde{\mu}_0$ and $\mathrm{Im}(\beta_n a) \simeq (ka^2\tilde{K}_0)^{1/2} \gg 1$, where $\tilde{K}_0$ is the average reflection coefficient of the nonlasant medium. For this case the effective Fresnel number is $F_K = 2\pi a^2 \tilde{K}_0/\lambda > 1$ with $L_{\mathrm{eff}} = \frac{1}{2}\tilde{K}_0$.

For the first-order Bragg reflection ($l=1$) typically $K_1 \simeq K_0/2 = 5\times 10^3$ cm^{-1} for channeling crystals, e.g., silicon and diamond.[6] Reflection guiding can be maintained by a surrounding medium of the same crystal, where Bragg reflections are avoided by impurities or dislocations, and $\tilde{K}_0 = K_0 > K_0 - K_1, \mu_0$. Another possibility for guiding is to use a surrounding medium with a higher atomic number with $\tilde{K}_0$ or $\tilde{\mu}_0$ of the order of 10^4 cm^{-1} and $L_{\mathrm{eff}} \simeq 1\ \mu$. The beam radius for guiding should be $a > (\lambda L_{\mathrm{eff}}/\pi)^{1/2}$ and for $\lambda = 3$ Å, $a > 100$ Å. Thus radiation guiding and amplification can be obtained for high current density of 10^5 A/cm^2 and for very low total current in the range of 10 μA.

For the case that the surrounding nonlasant medium is the same as the lasant medium (includes Bragg reflections but with no gain), then it is possible to write for this region a similar equation to Eq. (19), where $g_\pm = 0$ and α_n is replaced by β_n. Substituting it in Eq. (19), using the continuity conditions of the fields at the boundary and the strong reflection conditions ($|q_n L| \ll 1$, $K_0 L \gg 1$), we find that the only guiding mechanism is the gain guiding with $\mathrm{Im}(\beta_n a) \simeq (ka^2 g/2)^{1/2} \gg 1$. Here the effective Fresnel number $F_g = \pi a^2 g/\lambda > 1$ with $L_{\mathrm{eff}} = 1/g$. The beam radius for gain guiding is $a > (\lambda/\pi g)^{1/2}$ and for $\lambda = 3$ Å, $g = 10^{-2}$ cm^{-1} then $a > 10\ \mu$m, and gain guiding increases the requirements on the total beam current.

IV. GUIDING IN A ONE-PASS CHANNELING X-RAY LASER

The equation of motion for a one-passage amplifier with no resonance Bragg reflections is obtained from Eq. (12) $\epsilon \equiv \epsilon_+$, $\epsilon_- = 0$, $\nu_\pm = 0$,

$$-\frac{i}{2k}\nabla_\perp^2 \epsilon + \frac{\partial}{\partial z}\epsilon - (g_+ - i\delta - \nu_0)\epsilon = 0 , \tag{33}$$

where for a square well profile $g_- = g$, $\nu_0 = \mu_0 + iK_0$ for the lasant region $|x| < a$ and $|y| < a$, and $g_+ = 0$, $\nu_0 = \tilde{\nu}_0 = \tilde{\mu}_0 - i\tilde{K}_0$ out of the amplification region. Following the treatment of Sec. III, the eigenmodes solutions can be written as

$$\epsilon^{(n,m)}(\rho, z) = e^{q_{n,m} z} U^{(n)}(x) U^{(m)}(y) , \tag{34}$$

where $q_{n,m} = (q_n + q_m)/2$. The mode equation for $U^{(n)}(x)$ is

$$\left[-\frac{i}{k}\frac{d^2}{dx^2} + q_n - g + i\delta + \nu_0\right] U^{(n)}(x) = 0 . \tag{35}$$

The symmetric solutions of Eq. (35) are

$$U^{(n)}(x) = \begin{cases} A(e^{i\alpha_n x} + e^{-i\alpha_n x}), & |x| \le a \\ Be^{i\beta_n x}, & x \ge a . \end{cases} \tag{36}$$

The relations between q_n, α_n, and β_n are similar to Eqs. (19)–(21) and are given by the relations

$$q_n - g + i\delta + \nu_0 + i\frac{\alpha_n^2}{k} = 0 , \tag{36a}$$

$$q_n + i\delta + \tilde{\nu}_0 + i\frac{\beta_n^2}{k} = 0 , \tag{36b}$$

$$\tan(\alpha_n a) = -i\frac{\beta_n}{\alpha_n} , \tag{36c}$$

with the guiding condition $\mathrm{Im}(\beta_n a) \gg 1$.

The guiding states are obtained for $|\alpha_n/\beta_n| \ll 1$ and from Eq. (36c) $\alpha_n a = (n + \frac{1}{2})\pi$. From Eq. (36a) the eigenvalues q_n are

$$q_n = g - \mu_0 - i\delta - iK_0 - i\frac{\pi^2}{a^2}(n + \tfrac{1}{2})^2 . \tag{37}$$

The gain factor of state (n,m) is $g_{n,m} = q_{n,m} + q_{n,m}^*$. For the guiding states $g_{n,m} = 2(g - \mu_0)$ and the amplification factor g should be larger than the average absorption μ_0.

From Eqs. (36a) and (36b) we have the relation

$$\nu_0 - \tilde{\nu}_0 - g + i\frac{\alpha_n^2}{k} - i\frac{\beta_n^2}{k} = 0 , \tag{38}$$

and for $|\alpha_n/\beta_n| \ll 1$ the solution for β_n is

$$\beta_n = [ik(g + \tilde{\mu}_0 - \mu_0) - k(\tilde{K}_0 - K_0)]^{1/2} . \tag{39}$$

In Eq. (39) there are three mechanisms for radiation guiding, where $\mathrm{Im}(\beta a) \gg 1$ independent of the system length. The absorption guiding is obtained for $\tilde{\mu}_0 > |g - \mu_0|$, $|\tilde{K}_0 - K_0|$, and $\mathrm{Im}(\beta a) \simeq (ka^2\tilde{\mu}_0/2) \gg 1$ with an effective Fresnel number $F_\mu = \pi a^2 \tilde{\mu}_0/\lambda > 1$. We obtain reflection guiding for $\tilde{K}_0 > K_0$, $|g + \tilde{\mu}_0 - \mu_0|$, and $\mathrm{Im}(\beta a) \simeq (ka^2\tilde{K}_0) \gg 1$, with an effective Fresnel number $F_K = 2\pi a^2 \tilde{K}_0/\lambda > 1$. The absorption or reflection guiding conditions in a one-pass channeling x-ray laser can only be maintained by a surrounding medium of larger atomic number, where $\tilde{K}_0$ or $\tilde{\mu}_0$ are larger than the lasant medium. Radiation guiding and amplification can be maintained for $\lambda = 3$ Å, $a > 100$ Å with $\tilde{\mu}_0$ and $\tilde{K}_0$ of the order of 10^4 cm^{-1}.

Gain guiding is obtained in Eq. (39) for $g > |\tilde{\mu}_0 - \mu_0|$, $|\tilde{K}_0 - K_0|$, and $\mathrm{Im}(\beta a) \simeq (ka^2 g/2)^{1/2} \gg 1$, with an effective Fresnel number $F_g = \pi a^2 g/\lambda > 1$. The beam radius for gain guiding should be $a > (\lambda/\pi g)^{1/2}$. For $\lambda = 3$ Å and $a \sim 100$–1000 Å, $g \ggg 1$ cm^{-1}. Thus gain guiding in very small beam radius can be obtained only by a further large increase in the current density.

V. DISCUSSION

In order to obtain significant gain from induced emission the current density in a DFB scheme should be high (10^4–10^5 A/cm^2). One of the concerns is the survival of the crystal. We consider heating of a diamond crystal by

a beam of 20 MeV, a current density of $J=10^4$ A/cm^2, and a pulse duration of $\Delta t=1$ nsec. The temperature change is $\Delta T=n_b c\Delta t\Delta\epsilon/c_V\rho$, where $\rho=2.55$ g/cm^3 (crystal density), $n_b=J/ec=2\times10^{12}$ cm^{-3} (beam density), $c_V=0.12$ cal/g K (specific heat), and $\Delta\epsilon=2.2$ MeV cm^2/g (electron energy loss[14]). The result is $\Delta T=40$ K and the heating is relatively low. The rms vibrational amplitude of the atoms scales with temperature as $1+T/T_D$, where T_D is the Debye temperature. Diamond has a very high Debye temperature (~2000 K), so even increasing the crystal temperature by 400 K increases the one-dimensional thermal vibration amplitude from 0.042 to 0.049 Å. Thus in diamond it is possible to increase the beam density or the pulse duration by an order of magnitude without an important effect on the crystal periodicity. The heating considered here is an upper bound because not all energy loss is coupled to the narrow lasing medium and part of it diffuses out. This may be the reason that an electron microscopy dc beam with a current density of 10^6 A/cm^2 does not destroy the emitter. Heating may be a problem for constant current accelerators that are usually employed for channel radiation measurement, but is not a problem for a short beam pulse of several nanoseconds and a cooled crystal with relatively high Debye temperature.

In such beams the total current can be very small (10 μA) and the transverse dimension $a\sim100-1000$ Å. Here radiation guiding in the amplification medium is important. In a system with $L=0.1$ cm, $\lambda=3$ Å the Fresnel spatial guiding is for $F_0=\pi a^2/\lambda L\gg1$ and $a>1$ μm. Thus Fresnel guiding exists for relatively higher currents of an order of 1 mA. The gain guiding can be obtained for $F_g=\pi a^2 g/\lambda>1$. This guiding is not practical because it impose a further increase in the gain or current density. In a DFB scheme it is possible to consider radiation guiding by surrounding the lasant channeling medium by a nonlasant medium. The surrounding medium can be of the same channeling crystal, where Bragg reflections are avoided by impurities or dislocations, or by a surrounding medium with a higher atomic number. In such a system reflection guiding and absorption guiding by the nonlasant regions can maintain the amplification of radiation modes in the lasant regions independent of the system length or gain factor. The guiding can be maintained for $F=\pi a^2/\lambda L_{\rm eff}>1$, where the effective length $L_{\rm eff}\sim1/\tilde{K}_0$ or $1/\tilde{\mu}_0$, with $\tilde{K}_0$ and $\tilde{\mu}_0$ the average reflection or absorption coefficient of the nonlasant medium, respectively.

It is possible to show by using the methods of Sec. III that the radiation guiding mechanisms in the x and y directions can be of different types. Thus it can be useful to consider a planar superlattice crystal with lasant channeling regions surrounded by nonlasant regions transverse to the beam propagation, where the lasant region dimension is of an order of 100 Å. Radiation guiding by reflection or absorption can be maintained in that transverse direction by the nonlasant regions. The guiding in the other transverse dimension can be Fresnel guiding ($F_0\gg1$) in a range of 1 μm. Thus radiation guiding in a beam of dimension (100 Å)$\times$(1 μm) can be maintained with a low beam current of 10 μA. The interaction of the beam with a lasant domain can be obtained by small scanning of the beam on the crystal surface.

The number of photons emitted in the spontaneous stage can be approximate from an emission of 10^{-3} photons/electron cm.[2] For a 10-nsec beam pulse, current density of 10^5 A/cm^2, beam radius 1 μm, and cavity length of 0.1 cm, the number of emitted photons is 2×10^4. In the stimulated emission stage the number of photons can be increased by several orders of magnitude if saturation can be attained. In this case, the number of photons is of the order of the number of electrons passing the cavity, which is 10^8. For x-ray laser application, as holographic imaging of biological systems, the sufficient number of coherent photons is 10^3.

High-current-density field emission beam sources (10^6 A/cm^2) with very low emittance ($G\,10^{-8}$ rad cm) and total current (10 nA) are dc sources used in scanning electron microscopy. In order to achieve an x-ray laser based on DFB scheme, it is interesting to consider an accelerator with such an electron source. If the source is pulsed with a pulse length of about 10 nsec, it is plausible that the current can be increased by a factor of 10^3 without increasing the emittance.

ACKNOWLEDGMENTS

We wish to acknowledge Professor Marshall Rosenbluth and Professor Amnon Fisher for useful discussions. This work was supported by the Naval Research Laboratory and the Strategic Defense Initiative Organization.

*Visiting scientist on leave from the Nuclear Research Center, Negev, P.O. Box 9001, Beer Sheva, Israel.

[1] J. U. Andersen, E. Bonderup, and R. H. Pantell, Ann. Rev. Nucl. Part. Sci. **33**, 453 (1983); V. V. Beloshitsky and F. F. Komarov, Phys. Rep. **93**, 117 (1982); G. Kurizki and J. K. McIver, Phys. Rev. B **32**, 4358 (1985).

[2] R. K. Klein *et al.*, Phys. Rev. B **31**, 68 (1985); B. L. Berman, B. A. Dahling, S. Datz, J. O. Kephart, R. K. Klein, R. H. Pantell, and H. Park, Nucl. Instrum. Methods B **10/11**, 611 (1985).

[3] V. V. Beloshitsky and M. A. Kumakhov, Phys. Lett. A **69**, 247 (1978).

[4] G. Kurizki, M. Strauss, J. Oreg, and N. Rostoker, Phys. Rev. A **35**, 3424 (1987).

[5] V. H. Ohtsuki, Nucl. Instrum. Methods B **2**, 80 (1984).

[6] M. Strauss, P. Amendt, N. Rostoker, and A. Ron, Appl. Phys. Lett. **52**, 866 (1988).

[7] J. F. Hainfeld, Scanning Electron Microsc. **1**, 591 (1977).

[8] D. Marcuse, *Light Transmission Optics* (Van Nostrand-Reinhold, New York, 1972), pp. 275–282.

[9] B. W. Batterman, Rev. Mod. Phys. **36**, 681 (1964); L. V. Azaroff, *Elements of X-Ray Crystallography* (McGraw-Hill,

New York, 1968).
[10]M. Strauss, P. Amendt, H. U. Rahman, and N. Rostoker, Phys. Rev. Lett. **55**, 406 (1985); M. Strauss, Phys. Rev. A **38**, 1358 (1988).
[11]H. Kogelnik and C. V. Shank, Appl. Phys. Lett. **18**, 152 (1971); J. Appl. Phys. **43**, 2327 (1972).
[12]B. W. Batterman, Phys. Rev. **126**, 1461 (1962); B. W. Batterman and D. R. Chipman, *ibid.* **127**, 690 (1962); J. Appl. Phys. **34**, 2716 (1963); H. Wagenfeld, *ibid.* **33**, 2907 (1962).
[13]N. W. Ashcroft and N. D. Mermin, *Solid State Physics*, (Holt, Rinehart and Winston, New York, 1976), pp. 780–795.
[14]L. Pages, E. Bertel, H. Joffre, and L. Sklavenitis, At. Data **4**, 15 (1972).